



041IC - Should I Order a PET Scan?
**Integrating Molecular Imaging into Urologic
Oncology Clinical Practice: Current
Approaches and Future Opportunities**

Sunday, May 17

Faculty

Marc A. Bjurlin, DO

Tracy Rose, MD

Spencer Behr, MD

Michael A. Gorin, MD

ATTENTION: You are prohibited from using or uploading content you accessed through this activity into external applications, bots, software, or websites, including those using artificial intelligence technologies and infrastructure, including deep learning, machine learning and large language models and generative AI.



DETAILS

RELATIONS



Journal of Urology

Volume 211, Issue 6

Jun 2024

ARTICLE

Advances in Molecular Imaging for Renal Tumors

[View article page](#)

Zhuo Tony Su, Nirmish Singla and Mohammad E. Allaf



Check for updates

© 2024 by American Urological Association Education and Research, Inc.

Publisher Wolters Kluwer

ISSN 0022-5347

Online 3, 2024

Print 2024

**Table.** Representative Radiotracers Targeting Membranous Receptors and Metabolic Pathways of Renal Tumors

Radiotracer	Receptor/metabolic pathway targeted	Indications ^{1,9}
Tracers targeting membranous biomarkers		
cG250 (girentuximab)	mAb ligand for CA-IX	Diagnosis of primary RCC, detection of metastatic RCC, and assessment of response to TKI
VM4-037	Small-molecule ligand for CA-IX	Preclinical data suggest utility for detection of metastatic RCC
XYIMSR-06	Small-molecule ligand for CA-IX	Improved pharmacokinetics than other radiotracers targeting CA-IX; preclinical data suggest utility for diagnosis of primary RCC and detection of metastatic RCC; compatible with SPECT/CT
⁶⁸ Ga-PSMA-11	Small-molecule ligand for PSMA	Detection of metastatic RCC
¹⁸ F-PSMA-1007	Small-molecule ligand for PSMA	Potential utility for diagnosis of primary RCC, detection of metastatic RCC, and assessment of response to TKI and ICI
¹⁸ F-DCFPyL	Small-molecule ligand for PSMA	Detection of metastatic RCC
⁸⁹ Zr-bevacizumab	mAb ligand for VEGFA	Assessment of response to antiangiogenic treatment
⁸⁹ Zr-atezolizumab	mAb ligand for PD-L1	Assessment of response to ICI
Tracers targeting metabolic pathways		
¹⁸ F-FDG	Glucose uptake and phosphorylation	Surveillance for recurrent and metastatic RCC, and assessment of response to TKI and ICI
^{99m} Tc-sestamibi	Uptake in cells with high mitochondrial content and low MDR pump expression	Differentiation of renal oncocytomas and HOCTs from other renal masses
¹¹ C-acetate	Lipid synthesis	Diagnosis of primary RCC
¹¹ C-choline	Cellular membrane synthesis	Diagnosis of primary RCC
¹¹ C-methionine	Amino acid metabolism	RCC staging and prognosis prediction
¹⁸ F-(2S,4R)-4-fluoroglutamine	Amino acid metabolism	Detection of glutamine-dependent RCC

Abbreviations: CA-IX, carbonic anhydrase IX; FDG, fluoro-2-deoxy-d-glucose; HOCT, hybrid oncocyctic/chromophobe tumor; ICI, immune checkpoint inhibitor; mAb, monoclonal antibody; MDR, multidrug resistance; PD-L1, programmed cell death ligand-1; PSMA, prostate-specific membrane antigen; RCC, renal cell carcinoma; SPECT/CT, single-photon emission CT/CT; TKI, tyrosine kinase inhibitor; VEGFA, vascular endothelial-derived growth factor A.

85.9% for detecting primary ccRCC lesions, superior to 75.5% and 46.8% for CT.⁵ Since ¹²⁴I-labeled radiotracers tend to accumulate in the thyroid, ⁸⁹Zr-labeled cG250 has been developed. Recently, a prospective, multicenter, phase 3 study (ZIRCON) evaluated the utility of ⁸⁹Zr-cG250 for diagnosing primary ccRCC. In 284 patients, ⁸⁹Zr-cG250 achieved a sensitivity of 85.5% and specificity of 87.0% for identifying primary ccRCC lesions, exceeding the study's predetermined sensitivity and specificity targets.⁶ Furthermore, ⁸⁹Zr-cG250 has shown utility for detecting metastatic RCC. In a prospective study of 42 patients with metastatic ccRCC, ⁸⁹Zr-cG250 PET/CT combined with CT detected 91% of metastatic lesions, significantly higher than 56% by CT alone and 84% by combined ¹⁸F-FDG PET/CT and CT.²

Currently, efforts are underway to develop and validate radiotracers of lower molecular weights than mAb ligands, in order to achieve better penetration to solid tumors, shorter circulation time, and therefore more rapid attainment of a high tumor-to-blood ratio convenient for real-world use. VM4-037

dual-motif small-molecule ligand for CA-IX, is particularly promising. In RCC xenograft models, ⁶⁴Cu-XYIMSR-06 PET/CT demonstrated superior pharmacokinetics compared to existing radiotracers targeting CA-IX and most notably achieved an average tumor-to-kidney ratio of 7.1 at 24 hours post injection.⁸ Therefore, ⁶⁴Cu-XYIMSR-06 may be the first small-molecule ligand for CA-IX appropriate for diagnosing primary RCC. Clinical evaluation of ⁶⁴Cu-XYIMSR-06 is ongoing.

SPECT/CT RADIOTRACERS

All radiotracers discussed thus far have been applied in PET/CT imaging. Another opportunity in molecular imaging of renal tumors is to develop radiotracers for use with SPECT/CT. Currently, PET/CT remains expensive and not widely available, whereas SPECT/CT requires low costs and can be performed in most hospitals. A successful example of a SPECT/CT radiotracer employed for renal tumor imaging is ⁹⁹Tc-sestamibi, a widely used radiotracer approved for imaging of multiple



JU Insight

Comparing Magnetic Resonance Imaging and Prostate-Specific Membrane Antigen–Positron Emission Tomography for Prediction of Extraprostatic Extension of Prostate Cancer and Surgical Guidance: A Prospective Nonrandomized Clinical Trial

Clinton D. Bahler, Isamu Tachibana, Mark Tann, et al.

Correspondence: Clinton D. Bahler (cdbahler@iu.edu).

Full-length article available at <https://doi.org/10.1097/JU.0000000000004032>.

Study Need and Importance: Advanced prostate imaging with MRI has greatly increased personalized medicine by shifting to a lesion-based approach. This lesion-based approach has enabled targeted biopsy and refinement of surgical plans for both focal therapy and radical prostatectomy. For radical prostatectomy, predicting extraprostatic extension (EPE) is critical to safely select men for nerve-sparing surgery and continence-sparing approaches such as Retzius sparing. However, enthusiasm for MRI has been tempered with real-world sensitivity for EPE near 60%. Prostate cancer is difficult to image with anatomy-based modalities (ultrasound, CT, MRI, etc). ⁶⁸Ga–prostate-specific membrane antigen–11 positron emission tomography CT (PSMA-PET) offers the advantage of molecularly targeted tracers with high sensitivity for lesions likely to have EPE (Gleason $\geq 4+3$). We hypothesized that PSMA-PET, when compared to MRI, would have increased sensitivity for EPE.

What We Found: Fifty patients were prospectively enrolled, and the population was weighted toward EPE (44%) and high-risk with Gleason grade 3 + 4 (30%), 4 + 3 (30%), and 4 + 4/4 + 5 (38%). Radiologists knew patients were scheduling for prostatectomy, but they reviewed anonymized images with no clinicopathologic information (blinded). The sensitivity was higher for PSMA-PET when compared to MRI (86% vs 57%, $P = .03$), while specificity was similar. The PSMA-PET changed the surgical plan from nonnerve sparing to nerve sparing in 20 (40%)



Figure. This patient had PSA of 4.9, prostate size 48 cm³ (PSA density: 0.10), and Gleason biopsy worst core of 4 + 4. His final pathology showed Gleason 3 + 4 and pT3a. Gleason patterns 3 and 4 are listed by lesion. The MRI did not predict extraprostatic extension (EPE), while the ⁶⁸Ga–prostate-specific membrane antigen–11 positron emission tomography CT (PET) interpretation showed possible bilateral extraprostatic extension. Final pathology showed left-sided extraprostatic extension. NVB indicates neurovascular bundle.

cases and from nerve sparing to nonnerve sparing in 5 cases. The Figure demonstrates the ability of PSMA-PET to locate tumors near the prostate capsule at risk for EPE. The positive margin rate was not increased in patients with treatment change toward nerve-sparing.

Limitations: This is a single-institution study with expert radiology interpretations. Imaging accuracy could vary based on the quality of PET scanner and experience of the radiologists.

Interpretation for Patient Care: In this prospective trial, PSMA-PET resulted in higher sensitivity for EPE and increased the nerve-sparing rate during radical robotic prostatectomy without increasing positive margins.

Comparing Magnetic Resonance Imaging and Prostate-Specific Membrane Antigen–Positron Emission Tomography for Prediction of Extraprostatic Extension of Prostate Cancer and Surgical Guidance: A Prospective Nonrandomized Clinical Trial

Clinton D. Bahler,^{1*} Isamu Tachibana,^{1*} Mark Tann,² Katrina Collins,³ Jordan K. Swensson,² Mark A. Green,² Carla J. Mathias,² Yan Tong,⁴ Courtney Yong,¹ Ronald S. Boris,¹ Eric Brocken,³ Gary D. Hutchins,² Justin B. Sims,² Danielle V. Hill,² Nathaniel Smith,² Christopher Ferari,¹ Harrison Love,¹ and Michael O. Koch¹

¹Department of Urology, Indiana University, Indianapolis, Indiana

²Department of Radiology, Indiana University, Indianapolis, Indiana

³Department of Pathology, Indiana University, Indianapolis, Indiana

⁴Department of Statistics, Indiana University, Indianapolis, Indiana

Purpose: Survivors of surgically managed prostate cancer may experience urinary incontinence and erectile dysfunction. Our aim was to determine if ⁶⁸Ga–prostate-specific membrane antigen–11 positron emission tomography CT (PSMA-PET) in addition to multiparametric (mp) MRI scans improved surgical decision-making for nonnerve-sparing or nerve-sparing approach.

Materials and Methods: We prospectively enrolled 50 patients at risk for extraprostatic extension (EPE) who were scheduled for prostatectomy. After mpMRI and PSMA-PET images were read for EPE prediction, surgeons prospectively answered questionnaires based on mpMRI and PSMA-PET scans on the decision for nerve-sparing or nonnerve-sparing approach. Final whole-mount pathology was the reference standard. Sensitivity, specificity, positive predictive value, negative predictive value, and receiver operating characteristic curves were calculated and McNemar’s test was used to compare imaging modalities.

Results: The median age and PSA were 61.5 years and 7.0 ng/dL. The sensitivity for EPE along the posterior neurovascular bundle was higher for PSMA-PET than mpMRI (86% vs 57%, $P = .03$). For MRI, the specificity, positive predictive value,

Submitted November 21, 2023; accepted April 30, 2024; published May 24, 2024.

Funding/Support: This study was funded by donations from Al Christy Jr to the Indiana University Foundation prostate cancer research fund (Dr Bahler), American Cancer Society IRG Grant 16-192-31 (Dr Bahler), and NIH-NCI Grant R01CA202695 (Drs Hutchins and Green).

Conflict of Interest Disclosures: Drs Mathias and Green reported receiving funding from Five Eleven Pharmaceuticals. No other disclosures were reported.

Ethics Statement: This study received Institutional Review Board approval (IRB No. 11330).

Author Contributions:

Conception and design: Bahler, Tachibana, Green, Brocken, Hutchins, Koch, Boris, Tann.

Data analysis and interpretation: Tachibana, Swensson, Green, Mathias, Tong, Yong, Hutchins, Sims, Smith, Love, Koch.

Data acquisition: Bahler, Tachibana, Collins, Swensson, Green, Mathias, Yong, Brocken, Hutchins, Hill, Love, Koch, Boris, Tann.

Critical revision of the manuscript for scientific and factual content: Tachibana, Collins, Swensson, Green, Mathias, Yong, Hutchins, Sims, Smith, Love, Koch.

Drafting the manuscript: Bahler, Tachibana, Mathias, Tong, Yong, Brocken, Hill, Smith.

Statistical analysis: Bahler, Tachibana, Tong, Hutchins, Smith.

Supervision: Collins, Swensson, Green, Mathias, Yong, Hutchins, Sims, Koch.

Corresponding Author: Clinton D. Bahler, MD, MS, Department of Urology, Indiana University School of Medicine, 535 N Barnhill Dr, STE 420, Indianapolis, IN 46202 (cdbahler@iu.edu).

* Co-first authors.

negative predictive value, and area under the curve for the receiver operating characteristic curves were 77%, 40%, 87%, and 0.67, and for PSMA-PET were 73%, 46%, 95%, and 0.80. PSMA-PET and mpMRI reads differed on 27 nerve bundles, with PSMA-PET being correct in 20 cases and MRI being correct in 7 cases. Surgeons predicted correct nerve-sparing approach 74% of the time with PSMA-PET scan in addition to mpMRI compared to 65% with mpMRI alone ($P = .01$).

Conclusions: PSMA-PET scan was more sensitive than mpMRI for EPE along the neurovascular bundles and improved surgical decisions for nerve-sparing approach. Further study of PSMA-PET for surgical guidance is warranted in the unfavorable intermediate-risk or worse populations.

ClinicalTrials.gov Identifier: NCT04936334.

Key Words: pathology, PET scan, prostate cancer, prostatectomy, quality of life

SURGICAL resection of prostate cancer (PCa) involves the balance of resection to achieve negative margins and preserving sexual and urinary function.^{1,2} Patient satisfaction is often related to being cancer-free and maintaining normal urinary and erectile function.³⁻⁵ Preoperative imaging with multiparametric (mp) MRI to predict extraprostatic extension (EPE) of PCa has been unreliable.^{6,7} Finding a more accurate diagnostic imaging platform to detect the extent of PCa would be helpful in surgical planning.

Recently, ⁶⁸Ga-prostate-specific membrane antigen-11 positron emission tomography CT (PSMA-PET) scans have demonstrated higher sensitivity for EPE and the ability to detect more aggressive features.⁸⁻¹³ Herein, a prospective study was designed to compare mpMRI and PSMA-PET performance in EPE prediction in patients with intermediate- to high-risk disease. Using the final whole-mount pathology after surgical resection as a reference standard, our aim was to determine if PSMA-PET added value in preoperative planning to help surgeons better define the nerve-sparing or nonnerve-sparing approach.

METHODS

Patient Selection

With Institutional Review Board approval (IRB No. 11330, NCT04936334), we enrolled patients in a prospective, pilot, single-arm, single-institution clinical trial. All enrolled patients were diagnosed with intermediate-risk or worse PCa by the National Comprehensive Cancer Network guidelines and elected radical prostatectomy (RP). One patient was enrolled due to concern for EPE on MRI that did not meet eligibility criteria due to 3 + 3 Gleason grade. We defined patients with unfavorable intermediate-risk disease as having any grade Gleason score 4 + 3 = 7 disease, or $\geq 50\%$ positive cores of Gleason score 3 + 4 = 7 disease in accordance with guidelines.¹⁴ This was recorded for both whole gland and per side (left and right).

Radiology Interpretation

Included patients received a mpMRI within 6 months of surgery and a subsequent PSMA-PET with a 4.95 ± 0.10 mCi (183.2 ± 0.4 MBq) dose of ⁶⁸Ga-PSMA-11 (radiochemical purity = $99.6 \pm 0.4\%$).^{15,16} PSMA-PETs were

obtained on a Siemens Biograph Vision camera and reconstructed with the manufacturer's 3D Iterative (OSEM 2i5s) algorithm with time-of-flight.

Our dedicated radiology team included a board-certified nuclear medicine specialist (M.T.) who read all PSMA-PETs, and a fellowship-trained MRI radiologist (J.K.S.) read all mpMRIs. Image interpretation evaluated EPE likelihood at 4 locations deemed to be important for surgical guidance: (1) bladder neck, (2) posterior hemisphere along right nerve bundle, (3) posterior hemisphere along left nerve bundle, and (4) anterior apex near the dorsal venous complex and sphincter. Each reader was blinded to the other imaging modality and to all patient demographic and clinical parameters.

The PSMA-PET criterion for prostatic tumor involvement was focal or diffuse PSMA accumulation above the intraprostatic background. The PSMA-PET was considered positive for EPE when PET lesion contact length with prostate capsule, as measured on CT, was > 5 mm; this was chosen as whole-mount tissue sections were uniformly 5 mm in thickness. The core images of our clinical 3 T mpMRI protocol included small field of view T2-weighted images, diffusion-weighted imaging with apparent diffusion coefficient maps, and dynamic contrast-enhanced imaging. EPE detection by MRI has been previously validated using the sum of risk factors where a composite score of ≥ 1 is considered positive: curvilinear contact length of more than 1.5 cm, capsular bulge, and capsular irregularity.^{17,18}

Surgical Interpretation

Three surgeons (C.D.B., R.S.B., M.O.K.) included in the study completed questionnaires regarding planned resection approach (nonnerve-sparing vs nerve-sparing) and extended lymph node dissection (for concern of lymph node involvement) based on each imaging modality. A correct surgical approach was defined as selecting the appropriate nerve-sparing approach based on EPE. Partial nerve sparing was counted toward nonnerve sparing as this was performed due to concern of EPE. All surgeons were asked about surgical approach based on mpMRI prior to seeing the PSMA-PET. Subsequent questionnaires were completed following the PSMA-PET and immediately after surgery. The whole-mount pathology from the final surgical specimen was used as a gold standard to determine whether the preoperative imaging was predictive of EPE.

Primary and Secondary Outcomes

The primary objective of the study was to measure any difference in sensitivity and specificity for imaging prediction of posterior EPE at the left and right nerve bundle. This included calculation of sensitivity, specificity, positive predictive value (PPV), negative predictive value (NPV) of PSMA-PET, and mpMRI for EPE at the apex, bladder neck, and bilateral nerve bundles. Secondary end point included assessing the differential ability of the 2 imaging modalities to predict seminal vesicle invasion (SVI) and pelvic lymph node involvement was also studied. Additional analysis of surgeon surveys after both MRI and PET-CT were evaluated to determine the PSMA added value to mpMRI was more helpful for selecting patients for nerve-sparing or nonnerve-sparing approach.

Statistical Analysis

The sample size was based on the primary end point of identifying the sensitivity and specificity for PSMA-PET compared to mpMRI. A sample size of 50 patients generated 100 evaluable neurovascular bundles with each patient contributing 2. Based on preliminary data, the prevalence of EPE was estimated at 0.35.¹⁹ The sensitivity of PSMA-PET was anticipated to be 0.90. A sample size of 80 would provide a 2-sided 95% sensitivity confidence interval with a width of at most 0.23. The specificity of PSMA-PET was anticipated to be 0.75.¹⁹ A sample size of 80 would provide a 2-sided 95% specificity confidence interval with a width of at most 0.25. All calculations were based on the simple asymptotic method with continuity correction.

Descriptive statistics included medians and interquartile ranges were used for continuous variables, while frequency statistics were tabulated for categorical variables. Wilcoxon signed-rank test was used to compare medians between continuous clinical variables and χ^2 tests were used to compare categorical clinical variables to compare specimens with and without EPE. Proportions were tabulated for correct prediction based on radiologist and surgeon questionnaires for each imaging modality and compared using McNemar's test. Sensitivity, specificity, PPV, and NPV for PSMA-PET and mpMRI were calculated for EPE and compared with McNemar's test as well to assess any differences in imaging modalities. Statistical analysis was performed using SAS 9.4, and an α value of .05 was considered significant.

RESULTS

Patient Population and Demographics

Fifty-three patients meeting inclusion criteria were identified between June 2021 and July 2022 of whom 50 were enrolled (2 refused and 1 had concerns for metastases), with 100 neurovascular bundles (left and right side) and followed until final pathology resulted after surgery. Clinical and pathologic characteristics for all patients are summarized in Table 1. mpMRI and PSMA-PET imaging characteristics are listed, but notably did not have any significant differences between the pathologic EPE and no EPE groups, although a trend

was noted toward more aggressive features in the EPE group. There were 22 patients with pathologic EPE and 28 patients without pathologic EPE, and when considering both right and left posterior hemispheres of the prostate, there were 21 posterior hemispheres with EPE and 79 without EPE. Most patients were intermediate risk with either Gleason score 7 (3 + 4 or 4 + 3) on biopsy with a median PSA of 7.0 ng/mL (interquartile range: 5.5-8.7). Patients with EPE had significantly higher Gleason score on biopsy pathology ($P < .01$) and positive surgical margins ($P = .01$).

Comparison of Imaging

Table 2 compares the predictive testing ability of PSMA-PET and mpMRI with sensitivity, specificity, PPV, NPV, and area under the curve for the receiver operating characteristic curve. When considering both sides of the prostate for a total of 100 potential areas for EPE along the neurovascular bundles, PSMA-PET had higher sensitivity for EPE (0.87 vs 0.57, $P = .03$). The specificity was similar for both PSMA-PET and mpMRI (0.77 vs 0.73, $P = .49$). Receiver operating characteristic curve analysis for EPE demonstrated that for PSMA-PET, the area under the curve was 0.80 compared to 0.67 for mpMRI ($P = .07$). Figure 1 illustrates an example of one patient's mpMRI (with both a false-negative and positive on 2 lesions) and PSMA-PET with a comparison to the final whole mount.

A Sankey diagram (Figure 2) also highlights differences between PSMA-PET and mpMRI in predicting EPE. Patients were categorized as favorable (<50% of cores Gleason score $\leq 3 + 4$), or unfavorable disease (more than 50% of cores Gleason score $\geq 3 + 4$), on each prostate hemisphere. Of the 48 sides with favorable-risk disease on biopsy, only 2 patients had EPE. With favorable-risk disease, there were 6 false-positives with PSMA-PET compared to 7 with MRI, but no false-negatives were noted with either imaging modality (Supplementary Figure 2, <https://www.jurology.com>). For patients with unfavorable intermediate-risk disease or worse on biopsy, PSMA-PET had significantly higher sensitivity: mpMRI had an NPV of 0.71 (9 false-negatives) compared to NPV of 0.86 (3 false-negatives) for PSMA-PET. Although PSMA-PET had fewer false-negatives, mpMRI predicted a higher overall number of patients without EPE. In the same cohort of unfavorable-risk patients, the false-positive rate is much higher: mpMRI's PPV was 0.48 compared to PSMA-PET's PPV of 0.52. Supplementary Figure 1 (<https://www.jurology.com>) demonstrates cases where the MRI and PSMA-PET had disagreement with regard to EPE.

Referring to Table 2, the ability to predict EPE at the bladder neck and apex are reported; however, no

Table 1. Patient Characteristics Based on Extraprostatic Extension Status

Characteristics	Extraprostatic extension		P value
	No	Yes	
No.	28	22	
Age at surgery, median (IQR), y	61.5 (56.5, 66.5)	62.0 (58.0, 67.0)	.88
Family history of prostate cancer, No. (%)			.20
No	23 (82.1)	20 (90.9)	
Yes	5 (17.9)	1 (4.5)	
Unknown		1 (4.5)	
BMI, median (IQR), kg/m ²	28.7 (26.6, 33.5)	30.5 (25.4, 34.9)	.76
Race, No. (%)			.14
African American	5 (17.9)	1 (4.5)	
Caucasian	21 (75.0)	21 (95.5)	
Other	2 (7.1)		
PSA, median (IQR)	7.1 (4.9, 8.2)	6.9 (5.6, 9.2)	.57
PET noncancer SUVmax, median (IQR)	2.2 (1.9-3.2)	2.5 (2.1-3.1)	.22
PET dimension, median (IQR), cm	1.3 (1.0, 1.5)	1.7 (1.1, 2.3)	.13
PET SUVmean, median (IQR)	5.0 (3.3, 7.5)	5.8 (5.0, 9.6)	.14
PET SUVmax, median (IQR)	7.1 (4.0, 16.0)	9.7 (6.0, 13.5)	.19
PET contact length, median (IQR), cm	7.8 (4.5, 17.0)	12.0 (8.0, 18.0)	.33
PET primary score, No. (%)			.36
1	4 (14.3)	-	
2	1 (3.6)	1 (4.6)	
3	2 (7.1)	3 (13.6)	
4	13 (46.4)	9 (40.9)	
5	8 (28.6)	9 (40.9)	
MRI dimension, median (IQR), cm	1.4 (1.3, 2.0)	1.6 (1.5, 2.1)	.39
MRI contact length, median (IQR), cm	15.5 (10.5, 22.0)	16.0 (11.0, 20.0)	.73
MRI ADC, median (IQR)	582.0 (493.0, 753.0)	737.0 (551.0, 807.0)	.19
MRI PIRADS, No. (%)			.43
3	7 (25.0)	6 (27.3)	
4	16 (57.1)	9 (40.9)	
5	5 (17.9)	7 (31.8)	
Grade Group pathology, No. (%)			.11
1	1 (3.6)		
2	12 (42.9)	3 (13.6)	
3	7 (25.0)	8 (36.4)	
4	5 (17.9)	4 (18.2)	
5	3 (10.7)	7 (31.8)	
TNM pathology stage, No. (%)			< .01
T2	25 (89.3)		
T3a		12 (54.5)	
T3b	3 (10.7)	10 (45.5)	
Pelvic LN positive, No. (%)			.11
No	25 (89.3)	16 (72.7)	
Yes	2 (7.1)	6 (27.3)	
None removed	1 (3.6)		
Surgical margins, No. (%)			.01
Positive	3 (10.7)	9 (40.9)	

Abbreviations: ADC, apparent diffusion coefficient; IQR, interquartile range; LN, lymph node; PET, positron emission tomography; PIRADS, Prostate Imaging Reporting and Data System; SUVmax, maximum standardized uptake value; SUVmean, mean standardized uptake value.

patients had EPE at the bladder neck and only 1 patient had EPE at the apex. It is worth noting that 10 patients had SVI which mpMRI had 1.00 sensitivity, but the PSMA-PET only had 0.50 sensitivity ($P = .03$) and 0.93 specificity ($P = .25$). For lymph nodes, PSMA-PET had a sensitivity of 0.44 compared to 0% for mpMRI as the mpMRI did not identify any cases with lymph node involvement ($P = .05$).

Surgeon Questionnaires

Surgeons were also asked prior to RP whether a nerve-sparing or a nonnerve-sparing procedure would be performed based on EPE prediction of mpMRI, then subsequently asked on a separate

questionnaire based on EPE prediction of PSMA-PET. Forty-eight surveys were completed for PSMA-PET for analysis. As demonstrated in Table 3, the addition of PSMA-PET resulted in surgeons choosing the correct surgical plan more frequently when compared to the mpMRI-based plan alone ($P = .01$). When there was a discrepancy between PSMA-PET and mpMRI (27 sides in total), the added PSMA-PET allowed surgeons to correctly choose the appropriate nerve-sparing surgical procedure in 20 of the cases compared to 7 cases in favor of mpMRI ($P = .01$). In 22 of 27 sides (81%), surgeons elected to change from a nonnerve-sparing procedure to a nerve-sparing RP with the addition of PSMA-PET findings and were able to

Table 2. Sensitivity, Specificity, Positive Predictive Value, and Negative Predictive Value of MRI and ⁶⁸Ga-Prostate-Specific Membrane Antigen-11 Positron Emission Tomography CT in Preoperative Disease Staging

Outcome	Imaging modality	Sensitivity (95% CI)	Specificity (95% CI)	PPV (95% CI)	NPV (95% CI)	AUC (95% CI)
EPE at neurovascular bundle region, left and right (N = 100)	MRI	0.57 (0.36-0.78)	0.77 (0.68-0.86)	0.40 (0.22-0.58)	0.87 (0.79-0.95)	0.67 (0.55-0.79)
	PET	0.86 (0.71-1.00)	0.73 (0.64-0.83)	0.46 (0.31-0.62)	0.95 (0.90-1.00)	0.80 (0.70-0.89)
	Difference (95% CI) P value ^a	-0.29 (-0.54 to -0.03) .03	0.04 (-0.10 to 0.17) .49			-0.12 (-0.26 to 0.01) .07
Seminal vesicle invasion	MRI	1.00 (1.00-1.00)	1.00 (1.00-1.00)	1.00 (1.00-1.00)	1.00 (1.00-1.00)	1.00 (1.00-1.00)
	PET	0.50 (0.19-0.81)	0.93 (0.84-1.00)	0.63 (0.29-0.96)	0.88 (0.78-0.98)	0.71 (0.54-0.88)
	Difference (95% CI) P value ^a	0.50 (0.19-0.81) .03	0.07 (-0.01 to 0.16) .25			0.29 (0.12-0.46) < .01
Lymph node involvement	MRI	0.00 (0.00-0.00)	0.98 (0.93-1.00)	0.00 (0.00-0.00)	0.82 (0.71-0.92)	0.51 (0.49-0.54)
	PET	0.44 (0.12-0.77)	0.98 (0.93-1.00)	0.80 (0.45-1.00)	0.89 (0.80-0.98)	0.71 (0.54-0.88)
	Difference (95% CI) P value ^a	-0.44 (-0.77 to -0.12) .05	0.00 (-0.07 to 0.07) 1.00			-0.20 (-0.37 to -0.02) .03

Abbreviations: AUC, area under the curve; EPE, extraprostatic extension; NPV, negative predictive value; PET, positron emission tomography; PPV, positive predictive value. Bolded text indicates $\alpha \leq .05$.

^a McNemar's test was used to evaluate difference.

better predict in 19 of the cases. In the remaining 5 cases, surgeons elected to go from a nerve-sparing to a nonnerve-sparing RP but were only concordant with pathology in one of those cases. Importantly,

the positive margin rate was not increased in the 20 patients who went from a nonnerve-sparing to nerve-sparing approach, when compared to the overall study rate (25% vs 24%, $P = .89$). Notably,

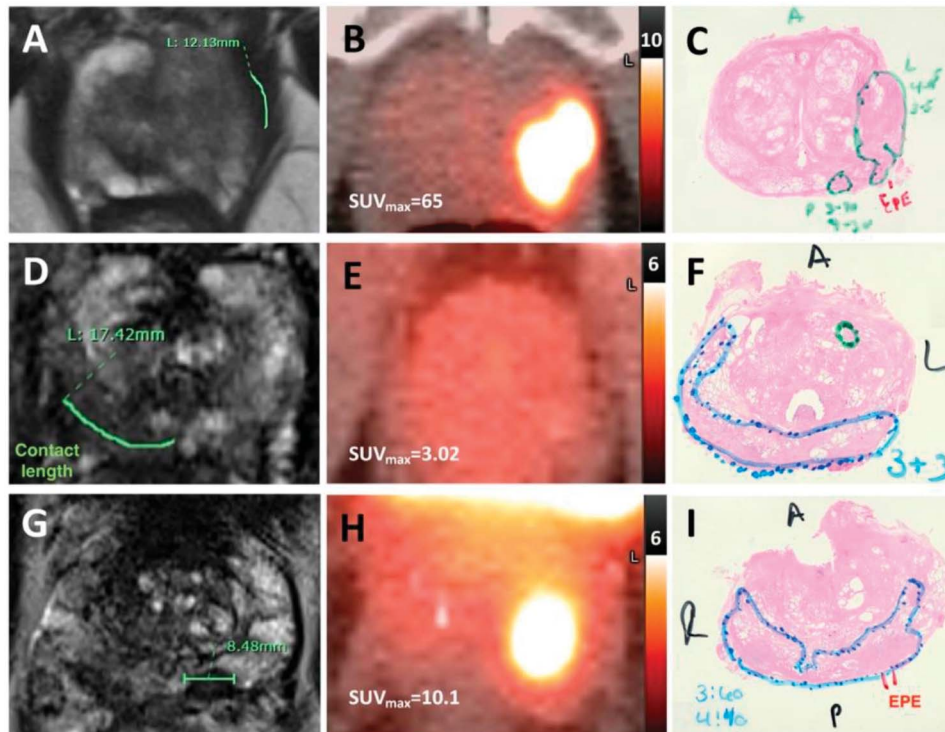


Figure 1. Comparison of multiparametric MRI, PSMA-PET (⁶⁸Ga-prostate-specific membrane antigen-11 positron emission tomography CT), and whole mount for 2 cases. The first case (A to C) demonstrates a 74-year-old with PSA 14.3 ng/mL and a 53-cm³ prostate (PSA density 0.27) with biopsy showing 4 + 4 prostate cancer (3 cores in left mid and apex). The MRI (A) was read as left anterior apical lesion without extraprostatic extension (EPE) at the neurovascular bundle while the PSMA-PET (B) was read as likely left-sided EPE at the neurovascular bundle. The final pathology (C) confirmed left EPE. The second case (apex: D-F, base: G-I) demonstrates a 66-year-old with PSA 6.8 ng/mL and a 42-cm³ prostate (PSA density 0.16) with biopsy showing 3 + 3 at the right apex and 4 + 3 at the base. The MRI (D) was read as right apical EPE, while the PSMA-PET (E) and final pathology (F) did not show EPE at the apex. The MRI (G) did not predict EPE at the base, while the PSMA-PET (H) and final pathology (I) showed EPE at the left base. SUVmax indicates maximum standardized uptake value.

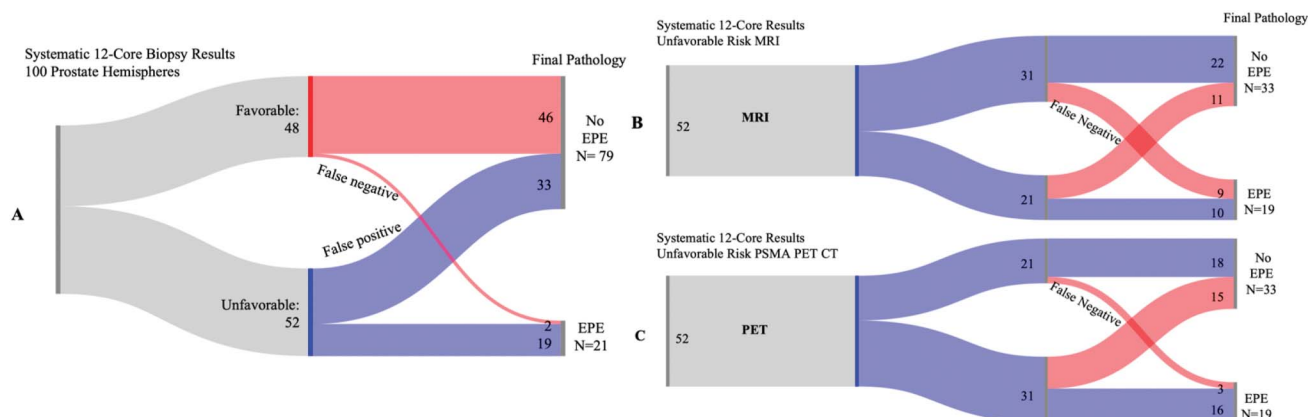


Figure 2. Sankey diagram of 50 patients evaluating each hemisphere (N = 100). Surgical planning for patient biopsy-classified as “favorable risk” (A) is unlikely to benefit from either advanced prostate imaging (multiparametric MRI or ⁶⁸Ga-prostate-specific membrane antigen–11 [PSMA] positron emission tomography [PET] CT)). However, for unfavorable-risk patients, PSMA-PET may improve further insight into extraprostatic extension (EPE) prediction as multiparametric MRI had 9 false-negatives compared to 3 false-negatives with PSMA-PET (B and C).

surgeons followed the recommended procedure from the radiologist in 0.89 of cases with PSMA-PET compared to 0.78 with mpMRI (*P* < .01).

DISCUSSION

In this prospective trial of patients undergoing RP who received both PSMA-PET and mpMRI, the PSMA-PET had higher sensitivity for predicting EPE. The PSMA-PET was helpful in selecting patients at low risk of EPE (NPV = 0.95) and resulted in 40% of patients having increased preservation of the neurovascular bundles. As highlighted by Figure 1, patients with favorable-risk disease on biopsy (Gleason score 3 + 3 = 6 or low volume 3 + 4 = 7) were nearly always free of EPE. Therefore, combined PSMA-PET and mpMRI imaging is unlikely to benefit surgical planning for favorable intermediate-risk disease. However, patients with unfavorable intermediate-risk disease or worse on biopsy (Gleason score 7, either ≥4 + 3 or ≥ 50% 3 + 4 cores per side) had significant treatment change with the PSMA-PET (*P* = .01). Additionally, mpMRI had higher sensitivity for SVI (*P* = .03).

The results of this study suggest PSMA-PET may have utility in surgical planning for unfavorable intermediate-risk or higher-risk patients, especially when considering a nerve-sparing approach.

Preoperative mpMRI is currently utilized for surgical planning, but studies have lacked reasonable accuracy in predicting organ-confined PCa.²⁰⁻²³ de Rooij et al published a meta-analysis of 75 studies and found the EPE 0.57 sensitivity and 0.91 specificity.⁶ Jansen et al reported on 430 patients undergoing mpMRI prior to prostatectomy and found a consistently low sensitivity rate (0.45).⁷ Although there are fewer reports with PSMA-PET, our group previously published on retrospective data and found that the sensitivity of EPE was significantly higher with PSMA-PET (0.90) compared to mpMRI (0.60, *P* = .02).¹⁹ Muehlemaier et al also found improved sensitivity for PSMA PET-MRI compared to mpMRI. For EPE, the sensitivity was 0.69 compared to 0.46 (*P* = .04) and the specificity was 0.75 (mpMRI) vs 0.67 (PET-MRI) (*P* = .19). For SVI, the sensitivity was 0.35 for mpMRI vs 0.55 for PET-MRI (*P* = .20) and 0.98 for mpMRI vs 0.94 for PET-MRI (*P* = .07).²⁴ In

Table 3. Surgeon Responses to Questionnaire for Surgical Plan Based on Multiparametric MRI and the Addition of ⁶⁸Ga-Prostate-Specific Membrane Antigen–11 Positron Emission Tomography CT

Outcome	Surgeon concordance based on MRI, No., proportion (95% CI of proportion)	Surgeon concordance based on addition of PET, No., proportion (95% CI of proportion) ^a	Difference in surgeon concordance based on MRI vs PET, proportion (95% CI of proportion)	<i>P</i> value ^b	Surgeon concordance during surgery, No., proportion (95% CI of proportion) ^c
EPE at neurovascular bundle region, left and right (N = 100)	65, 0.65 (0.55-0.74)	74, 0.77 (0.67-0.85)	−0.12 (−0.25 to 0.00)	.01	76, 0.76 (0.66-0.84)
Seminal vesicle invasion	39, 0.78 (0.64-0.88)	39, 0.81 (0.67-0.91)	−0.03 (−0.19 to 0.13)	1.00	42, 0.84 (0.71-0.93)
Lymph node involvement	40, 0.80 (0.66-0.90)	42, 0.88 (0.75-0.95)	−0.07 (−0.22 to 0.07)	.10	42, 0.84 (0.71-0.93)

Abbreviations: EPE, extraprostatic extension; PET, positron emission tomography.
^a N = 96 available data points for left + right; N = 48 available data points for other outcomes.
^b McNemar’s test was used to evaluate difference in surgeon concordance based on MRI vs PET.
^c Based on surgeon postoperative questionnaire.

contrast, studies have also found that mpMRI had a higher ability to detect EPE (0.79 vs 0.59, $P < .01$) or for SVI (0.84 vs 0.63, $P < .01$), although the vast majority of these patients had high-risk disease.²⁵ While both the Sonni²⁵ and Muehlematter²⁴ et al studies demonstrated consistent reliability between radiologists with mpMRI, there was significantly more variability with reading PSMA-PET in the Sonni et al study compared to mpMRI.

The high sensitivity in PSMA-PET may be related to its ability to detect regions with high percentage Gleason primary patterns 4 and 5.^{26,27} Several studies have demonstrated that increased standardized uptake value (SUV) signal intensity with PSMA-PET may be correlated with worse Gleason score.⁸⁻¹⁰ Demirci et al found that there was a correlation between maximum SUVs and grade groups for PCa (Pearson = 0.66) and those with high-risk disease had significantly higher maximum SUV than those with low-risk disease (18.9 ± 12.1 vs 7.16 ± 6.2 , $P < .01$).⁸ Perhaps the correlation of signal intensity with higher-risk disease may help surgical planning insofar as PSMA-PET may focus on clinically significant components within a larger tumor. Thus, PSMA-PET may allow for closer assessment of higher-risk parts of the tumor that may be associated with EPE thereby reducing false-negatives and higher sensitivity, despite lower soft tissue resolution of PSMA-PET imaging. This feature of identifying higher-risk tumors at risk for EPE with PSMA-PET, such that if a high-risk tumor did not show EPE on PSMA-PET, surgeons could reliably convert from nonnerve-sparing to nerve sparing, but not vice versa. The findings in this study are unique in that this is the first prospective study which allowed both radiologists and surgeons to predict EPE and the approach to nerve-sparing RP based on imaging. The PSMA-PET's high sensitivity allowed for the better surgical planning in sparing neurovascular tissue without compromising the positive margin rate. Specificity may be lower in this study as these patients had more favorable disease and were candidates for nerve-sparing.

Our results should be viewed in the context of certain limitations. While this is a prospective study, this study was conducted at a single institution with a dedicated mpMRI and nuclear imaging radiologist limiting interobserver variability. As shown in prior studies, better standardization of PSMA-PET (acquisition and interpretation) is necessary to minimize the variability with interpreting PSMA-PET. Additionally, standardization of mpMRI may also improve EPE prediction, as mpMRIs can frequently underestimate tumor size.²⁸⁻³⁰ Another potential cause of variability is that the PET-CT scanner used for these scans (Biograph Vision,

Siemens Healthcare) across different centers may contribute to difference in the quality of images. This could limit reproducibility at other sites; however, as there are updates to scanner capabilities, our analysis is highly relevant when considering standardization of PET-CT quality across centers. On a similar note, advances in prostate biopsy using transperineal techniques should be standardized as well to minimize variability across centers.

These limitations notwithstanding, this study highlights the adjunctive potential of PSMA-PET as a diagnostic tool in surgical planning for PCa. While mpMRI has previously been shown to be unreliable in predicting EPE, PSMA-PET may be useful due to the high sensitivity. As demonstrated in this study, when there were discrepancies between imaging modalities and surgeons elected to perform a nerve-sparing RP based on PSMA-PET, they were significantly more concordant with pathology. This utility of PSMA-PET in the preoperative setting may further improve standardization between radiologists and institutions. These findings should be replicated at other centers and with larger numbers; a nomogram with clinical factors such as Gleason score on biopsy, PSA serum levels, tumor size, and genomic data may further improve the ability to predict extension of disease to provide the appropriate surgical intervention for patients. A randomized trial is currently in year 2 out of 5 at our institution comparing PSMA-PET and mpMRI treatment planning for prostatectomy. Perhaps future studies to combine both PSMA-PET and mpMRI can have an additive benefit and improve sensitivity as demonstrated in studies to identify candidates for focal therapy.³¹

CONCLUSIONS

In this prospective trial, we enrolled 50 patients who underwent both mpMRI and PSMA-PET prior to RP. We found that the sensitivity (0.87 vs 0.57) for EPE was significantly better with PSMA-PET, although specificity was not significantly different (0.77 vs 0.73). When there was a discrepancy between mpMRI and PET CT scan (27 sides in total), the addition of PSMA-PET allowed the surgeon to appropriately choose surgical technique in 20 of the cases compared to 7 for mpMRI. While patients with biopsy-based favorable intermediate-risk disease were unlikely to benefit from the addition of mpMRI or PSMA-PET scan, there was added benefit from the use of advanced imaging in unfavorable intermediate-risk disease. Further studies using additional radiologists and surgeons are necessary to validate the generalizability of our findings and further evaluate the utility of PSMA-PET imaging for surgical planning.

REFERENCES

- Tewari A, Peabody JO, Fischer M, et al. An operative and anatomic study to help in nerve sparing during laparoscopic and robotic radical prostatectomy. *Eur Urol*. 2003;43(5):444-454. doi:10.1016/s0302-2838(03)00093-9
- Walsh PC. Radical prostatectomy for localized prostate cancer provides durable cancer control with excellent quality of life: a structured debate. *J Urol*. 2000;163(6):1802-1807. doi:10.1016/s0022-5347(05)67547-7
- Hoffman RM, Hunt WC, Gilliland FD, Stephenson RA, Potosky AL. Patient satisfaction with treatment decisions for clinically localized prostate carcinoma. Results from the Prostate Cancer Outcomes Study. *Cancer*. 2003;97(7):1653-1662. doi:10.1002/cncr.11233
- Wallis CJD, Glaser A, Hu JC, et al. Survival and complications following surgery and radiation for localized prostate cancer: an international collaborative review. *Eur Urol*. 2018;73(1):11-20. doi:10.1016/j.eururo.2017.05.055
- Wallis CJD, Zhao Z, Huang LC, et al. Association of treatment modality, functional outcomes, and baseline characteristics with treatment-related regret among men with localized prostate cancer. *JAMA Oncol*. 2022;8(1):50-59. doi:10.1001/jamaoncol.2021.5160
- de Rooij M, Hamoen EH, Witjes JA, Barentsz JO, Rovers MM. Accuracy of magnetic resonance imaging for local staging of prostate cancer: a diagnostic meta-analysis. *Eur Urol*. 2016;70(2):233-245. doi:10.1016/j.eururo.2015.07.029
- Jansen BHE, Oudshoorn FHK, Tijans AM, et al. Local staging with multiparametric MRI in daily clinical practice: diagnostic accuracy and evaluation of a radiologic learning curve. *World J Urol*. 2018;36(9):1409-1415. doi:10.1007/s00345-018-2295-6
- Demirci E, Kabasakal L, Sahin OE, et al. Can SUVmax values of Ga-68-PSMA PET/CT scan predict the clinically significant prostate cancer?. *Nucl Med Commun*. 2019;40(1):86-91. doi:10.1097/MNM.0000000000000942
- Uprimny C, Kroiss AS, Decristoforo C, et al. ⁶⁸Ga-PSMA-11 PET/CT in primary staging of prostate cancer: PSA and Gleason score predict the intensity of tracer accumulation in the primary tumour. *Eur J Nucl Med Mol Imaging*. 2017;44(6):941-949. doi:10.1007/s00259-017-3631-6
- Bahler CD, Johnson MM, Davicioni E, et al. Predictors of prostate-specific membrane antigen (PSMA/FOLH1) expression in a genomic database. *Urology*. 2020;144:117-122. doi:10.1016/j.urolgy.2020.06.025
- von Klot CAJ, Merseburger AS, Boker A, et al. ⁶⁸Ga-PSMA PET/CT imaging predicting intraprostatic tumor extent, extracapsular extension and seminal vesicle invasion prior to radical prostatectomy in patients with prostate cancer. *Nucl Med Mol Imaging*. 2017;51(4):314-322. doi:10.1007/s13139-017-0476-7
- Pienta KJ, Gorin MA, Rowe SP, et al. A phase 2/3 prospective multicenter study of the diagnostic accuracy of prostate specific membrane antigen PET/CT with ¹⁸F-DCFPyL in prostate cancer patients (OSPPEY). *J Urol*. 2021;206(1):52-61. doi:10.1097/JU.0000000000001698
- Hope TA, Eiber M, Armstrong WR, et al. Diagnostic accuracy of ⁶⁸Ga-PSMA-11 PET for pelvic nodal metastasis detection prior to radical prostatectomy and pelvic lymph node dissection: a multicenter prospective phase 3 imaging trial. *JAMA Oncol*. 2021;7(11):1635-1642. doi:10.1001/jamaoncol.2021.3771
- Schaeffer EM, Srinivas S, Adra N, et al. NCCN Guidelines® insights: prostate cancer, version 1.2023. *J Natl Compr Canc Netw*. 2022;20(12):1288-1298. doi:10.6004/jnccn.2022.0063
- Green MA, Eitel JA, Fletcher JW, et al. Estimation of radiation dosimetry for ⁶⁸Ga-HBED-CC (PSMA-11) in patients with suspected recurrence of prostate cancer. *Nucl Med Biol*. 2017;46:32-35. doi:10.1016/j.nucmedbio.2016.11.002
- Bjurlin MA, Carroll PR, Eggener S, et al. Update of the standard operating procedure on the use of multiparametric magnetic resonance imaging for the diagnosis, staging and management of prostate cancer. *J Urol*. 2020;203(4):706-712. doi:10.1097/JU.0000000000000617
- Turkbey B, Rosenkrantz AB, Haider MA, et al. Prostate imaging reporting and data system version 2.1: 2019 update of prostate imaging reporting and data system version 2. *Eur Urol*. 2019;76(3):340-351. doi:10.1016/j.eururo.2019.02.033
- Mehralivand S, Shih JH, Harmon S, et al. A grading system for the assessment of risk of extraprostatic extension of prostate cancer at multiparametric MRI. *Radiology*. 2019;290(3):709-719. doi:10.1148/radiol.2018181278
- Bahler CD, Green MA, Tann MA, et al. Assessing extra-prostatic extension for surgical guidance in prostate cancer: comparing two PSMA-PET tracers with the standard-of-care. *Urol Oncol*. 2023;41(1):48.e1-48.e9. doi:10.1016/j.urolonc.2022.10.003
- Wei JT, Barocas D, Carlsson S, et al. Early detection of prostate cancer: AUA/SUO guideline part II: considerations for a prostate biopsy. *J Urol*. 2023;210(1):54-63. doi:10.1097/JU.0000000000003492.
- Chuang AY, Nielsen ME, Hernandez DJ, Walsh PC, Epstein JI. The significance of positive surgical margin in areas of capsular incision in otherwise organ confined disease at radical prostatectomy. *J Urol*. 2007;178(4 Pt 1):1306-1310. doi:10.1016/j.juro.2007.05.159
- Kam J, Yuminaga Y, Krelle M, et al. Evaluation of the accuracy of multiparametric MRI for predicting prostate cancer pathology and tumour staging in the real world: an multicentre study. *BJU Int*. 2019;124(2):297-301. doi:10.1111/bju.14696
- Chandrasekar T, Denisenko A, Mico V, et al. Multiparametric MRI is not sufficient for prostate cancer staging: a single institutional experience validated by a multi-institutional regional collaborative. *Urol Oncol*. 2023;41(8):355.e1-355.e8. doi:10.1016/j.urolonc.2023.05.004
- Muehlethaler UJ, Burger IA, Becker AS, et al. Diagnostic accuracy of multiparametric MRI versus ⁶⁸Ga-PSMA-11 PET/MRI for extracapsular extension and seminal vesicle invasion in patients with prostate cancer. *Radiology*. 2019;293(2):350-358. doi:10.1148/radiol.2019190687
- Sonni I, Felker ER, Lenis AT, et al. Head-to-head comparison of ⁶⁸Ga-PSMA-11 PET/CT and mpMRI with a histopathology gold standard in the detection, intraprostatic localization, and determination of local extension of primary prostate cancer: results from a prospective single-center imaging trial. *J Nucl Med*. 2022;63(6):847-854. doi:10.2967/jnumed.121.262398
- Roberts MJ, Morton A, Donato P, et al. ⁶⁸Ga-PSMA PET/CT tumour intensity pre-operatively predicts adverse pathological outcomes and progression-free survival in localised prostate cancer. *Eur J Nucl Med Mol Imaging*. 2021;48(2):477-482. doi:10.1007/s00259-020-04944-2
- Scheltema MJ, Chang JI, Stricker PD, et al. Diagnostic accuracy of ⁶⁸Ga-prostate-specific membrane antigen (PSMA) positron-emission tomography (PET) and multiparametric (mp)MRI to detect intermediate-grade intra-prostatic prostate cancer using whole-mount pathology: impact of the addition of ⁶⁸Ga-PSMA PET to mpMRI. *BJU Int*. 2019;124(suppl 1):42-49. doi:10.1111/bju.14794
- Pooli A, Johnson DC, Shirk J, et al. Predicting pathological tumor size in prostate cancer based on multiparametric prostate magnetic resonance imaging and preoperative findings. *J Urol*. 2021;205(2):444-451. doi:10.1097/JU.0000000000001389
- Priester A, Natarajan S, Khoshnoodi P, et al. Magnetic resonance imaging underestimation of prostate cancer geometry: use of patient specific molds to correlate images with whole mount pathology. *J Urol*. 2017;197(2):320-326. doi:10.1016/j.juro.2016.07.084
- Turkbey B, Mani H, Aras O, et al. Correlation of magnetic resonance imaging tumor volume with histopathology. *J Urol*. 2012;188(4):1157-1163. doi:10.1016/j.juro.2012.06.011
- Geboers B, Meijer D, Counter W, et al. Prostate-specific membrane antigen positron emission tomography in addition to multiparametric magnetic resonance imaging and biopsies to select prostate cancer patients for focal therapy. *BJU Int*. 2024;133(suppl 4):14-22. doi:10.1111/bju.16207



Imaging Prostate Cancer: Clinical Utility of Prostate-Specific Membrane Antigen

David Kuppermann,¹ Jeremie Calais² and Leonard S. Marks^{1,*}

¹Department of Urology, David Geffen School of Medicine, University of California at Los Angeles, Los Angeles, California

²Ahmanson Translational Theranostics Division, Department of Molecular and Medical Pharmacology, David Geffen School of Medicine, UCLA, Los Angeles, California

Purpose: Our goal was to review the pathway and pertinent materials leading to approval of prostate-specific membrane antigen (PSMA) scanning by the U.S. Food and Drug Administration (FDA).

Materials and Methods: Beginning with the pivotal trials and working backward, we summarize the evolution of PSMA scanning, beginning with the discovery of the molecule, the mechanism of action to identify prostate cancer, the route to the present-day test and some of the major publications leading to each step of the sequence. From the thousands of PSMA articles listed on PubMed®, the present review is focused on the 4 large U.S. trials incorporating university studies of the gallium-68 compound and commercial studies of the fluorine-18 compound. The review further focuses on the role of PSMA scanning for both initial staging of prostate cancer and diagnosis of recurrent prostate cancer.

Results: PSMA is a transmembrane-bound glycoprotein which is overexpressed by 100–1,000-fold in prostate cancer cells. Preclinical PSMA studies at Cornell and Johns Hopkins in the 1990s were followed by early human studies in Germany in the early 2010s, then pivotal clinical trials at University of California, Los Angeles and University of California, San Francisco, leading to the first FDA approval in December 2020 (⁶⁸Ga-PSMA-11). In January 2021, a commercially available product (¹⁸F-DCFPyL) was approved on the basis of multisite registration trials (CONDOR and OSPREY). Sensitivity and specificity of PSMA scanning exceeds that of any other imaging method currently available for initial staging of prostate cancer and diagnosis of recurrent disease. The accuracy of PSMA scanning is attributed to the great image contrast (high signal-to-noise ratio), a property deriving from the high PSMA tracer uptake by prostate cancer cells. That property can be estimated quantitatively by a metric, the standardized uptake value. A follow-on PSMA compound, the theranostic lutetium-177, is currently pending FDA approval for treatment of metastases.

Conclusions: PSMA scanning is a disruptive technology that promises to transform the way prostate cancer is initially staged, recurrence is diagnosed and some advanced cases are treated.

Abbreviations and Acronyms

BCR = biochemical recurrence
 CT = computerized tomography
 FDA = U.S. Food and Drug Administration
 mpMRI = multiparametric magnetic resonance imaging
 MRI = magnetic resonance imaging
 NCCN® = National Comprehensive Cancer Network®
 PCa = prostate cancer
 PET = positron-emission tomography
 PPV = positive predictive value
 PSA = prostate specific antigen
 PSMA = prostate-specific membrane antigen
 RLT = radioligand therapy
 SUV = standardized uptake value
 UCLA = University of California, Los Angeles
 UCSF = University of California, San Francisco

Accepted for publication January 19, 2022.

Support: None.

Conflict of Interest: Dr. Marks is a consultant advisor to Exact Imaging and co-founder of Avenda Health; Dr. Calais reports prior consulting activities for Advanced Accelerator Applications, Blue Earth Diagnostics, Curium Pharma, GE Healthcare, IBA Radiopharma, Janssen Pharmaceuticals, Progenics Radiopharmaceuticals, Radiomedix and Telix Pharmaceuticals, outside of the submitted work. Dr. Calais is supported by the PCF (2020 Young Investigator Award 20YOUN05).

Ethics Statement: In lieu of a formal ethics committee, the principles of the Helsinki Declaration were followed.

* Correspondence: Department of Urology, David Geffen School of Medicine, University of California at Los Angeles, Wasserman Building, 300 Stein Plaza, 3rd floor, Los Angeles, California 90095 (telephone: 310-794-3070; FAX: 310-794-0987; email: lmarks@mednet.ucla.edu).

Key Words: prostate, prostatic neoplasms, glutamate carboxypeptidase, positron-emission tomography, molecular imaging

“BECAUSE of increased sensitivity and specificity, PSMA-PET/CT or PSMA-PET/MRI can serve as an...effective front-line imaging tool for initial staging and to detect biochemical recurrence of prostate cancer.”

NCCN Guidelines®, September 10, 2021¹

Prostate cancer (PCa) imaging based on prostate-specific membrane antigen (PSMA) is a disruptive innovation; its use has transformed diagnosis, staging and even treatment of PCa. PSMA is over-expressed by the great majority of PCa cells. PSMA-targeting small molecules can be bound to a radionuclide (eg gallium-68 or fluorine-18) and the conjugate can thus be visualized *in vivo* by scanning with positron-emission tomography (PET) scan. Anatomical localization of PSMA uptake is established by computerized tomography (CT) scanning overlay (PSMA PET/CT). Metastases and intra-prostatic cancer, not apparent by conventional imaging, may be seen. Use of PSMA PET/CT has redefined the patterns of PCa spread, resulting in a profound transformation of PCa management. PSMA PET/CT scanning was added to the National Comprehensive Cancer Network® (NCCN®) Guidelines® v1.2022 on September 10, 2021.¹ The following provides an overview of PSMA PET/CT imaging (not a systematic review), which was recently approved by the U.S. Food and Drug Administration (FDA) through use of the radiotracers ⁶⁸Ga-PSMA-11 and ¹⁸F-DCFPyL. Numerous systematic reviews (PRISMA) are available on PubMed® (75 as of January 2022). Herein we focus on the works most directly involved in the path to approval by the FDA.

BIOLOGY OF PSMA AND BASICS OF PSMA PET/CT IMAGING

PSMA (glutamate carboxypeptidase, folate hydro-lase) is a transmembrane-bound glycoprotein, native to prostate epithelial cells and overexpressed by 100–1,000-fold in PCa cells (fig. 1).² The normal function of PSMA remains unclear, but it may have a role in signaling and activating molecular pathways.³ When malignant transformation occurs, PSMA expression increases.^{4–7} The PSMA gene is located on the short arm of chromosome 11, a region not commonly deleted in PCa.⁸ The molecule has a unique 3-part structure consisting of an extracellular domain (707 amino acids), a transmembrane domain (24 amino acids) and an intracellular domain (19 amino acids; fig. 1).⁹ Since 95% of the molecule is extracellular, PSMA is readily accessible for binding of antibodies or low-molecular-weight ligands. PSMA-ligands can be labeled with radionuclides such as gallium-68 or fluorine-18 to

form a radiotracer. After injection, the PSMA-targeted radiotracer is rapidly cleared from the blood to the PSMA-binding sites, internalized and accumulated into the PSMA-expressing PCa cells.^{10,11}

Physiological PSMA expression may be seen in extraprostatic tissue, such as duodenum, small intestine, colon, kidney, salivary, lacrimal glands, nonmyelinated ganglia and the vascular supply of other cancers,¹² but not in the common sites of PCa metastasis (lymph nodes, bone).² Thus, with little background signal, allowing great contrast with PSMA-avid lesions, PET/CT visualization and localization of PCa is possible with accuracy not previously possible. A review by Maurer and associates, who were early investigators, provides extensive detail on the biology of PSMA.¹³

EVOLUTION OF PSMA-TARGETED IMAGING

Major milestones in the development of today's PSMA scan are shown in figure 2. The proximate forerunner of today's PSMA scan was ProstaScint® (capromab pentetide/7E11-C5).¹⁴ The ProstaScint scan (FDA approved 1996) employed a monoclonal antibody specific to the intracellular epitope of PSMA, radiolabeled with the gamma-emitter indium-111. Using gamma-camera imaging at 3 days of followup, the ProstaScint scan allowed visualization of PCa, including metastases. However, as the target was intracellular and ProstaScint could only bind to dying cells, the low signal/noise ratio reduced accuracy of ProstaScint scans. This and the poor image quality of indium-111 led to limited use and acceptance. The production of ProstaScint was discontinued in the U.S. in 2018.

In 1997, Neil Bander and others at Cornell discovered monoclonal antibodies to the extracellular epitope of PSMA (J591), conferring increased radiotracer uptake.^{15,16} At about the same time, Martin Pomper at Johns Hopkins reported that an enzyme in brain was homologous to PSMA and could be targeted with radiolabeled low-molecular weight ligands to image PCa.¹⁷ Thus was born modern interest in PSMA targeted scanning for diagnostic applications. Details of the preclinical discoveries are available elsewhere.^{18,19}

In 2012, researchers in Heidelberg, Germany reported the first patient imaged with a ⁶⁸Ga-labeled PSMA PET compound using the ligand PSMA-11.²⁰ Between 2012 and 2020 more than 1,700 studies on PSMA PET were published. On December 1st, 2020, nearly 10 years after its discovery, ⁶⁸Ga-PSMA-11 was cleared by the FDA as the first PSMA-targeted radiopharmaceutical for PET imaging of PCa.²¹ The FDA approval was originally restricted to the 2 centers where the ⁶⁸Ga-PSMA-11 radiotracer was manufactured in the pivotal trials (University of California, Los

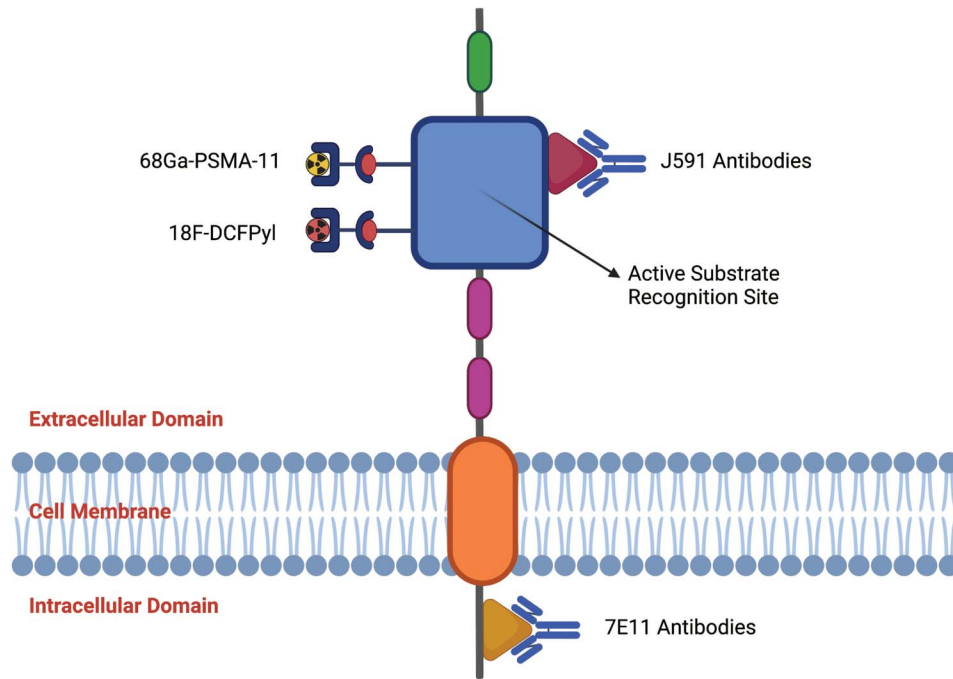


Figure 1. Molecular structure of PSMA. The transmembrane molecule consists of 3 parts: a short intracellular domain (19 amino acids), a transmembrane domain (24 amino acids) and a long extracellular domain (707 amino acids). The extracellular domain contains an active substrate-recognition site (blue square) which is targeted by the PSMA ligands, eg ^{68}Ga -PSMA-11 and ^{18}F -DCFPyl. ^{68}Ga -PSMA-11 and ^{18}F -DCFPyl attach to the extracellular epitope of the PSMA, like the J591 antibodies. During binding, a process of internalization occurs, resulting in intracellular accumulation of the bound radioligand.¹³

Angeles [UCLA] and University of California, San Francisco [UCSF]). However, widespread availability of PSMA PET imaging is expected, following FDA

clearance of the first commercially available PSMA PET radiotracer (Pylarify®, piflufolstat-18, Progenics/Lantheus) in May 2021.²² The 4 studies of PSMA PET

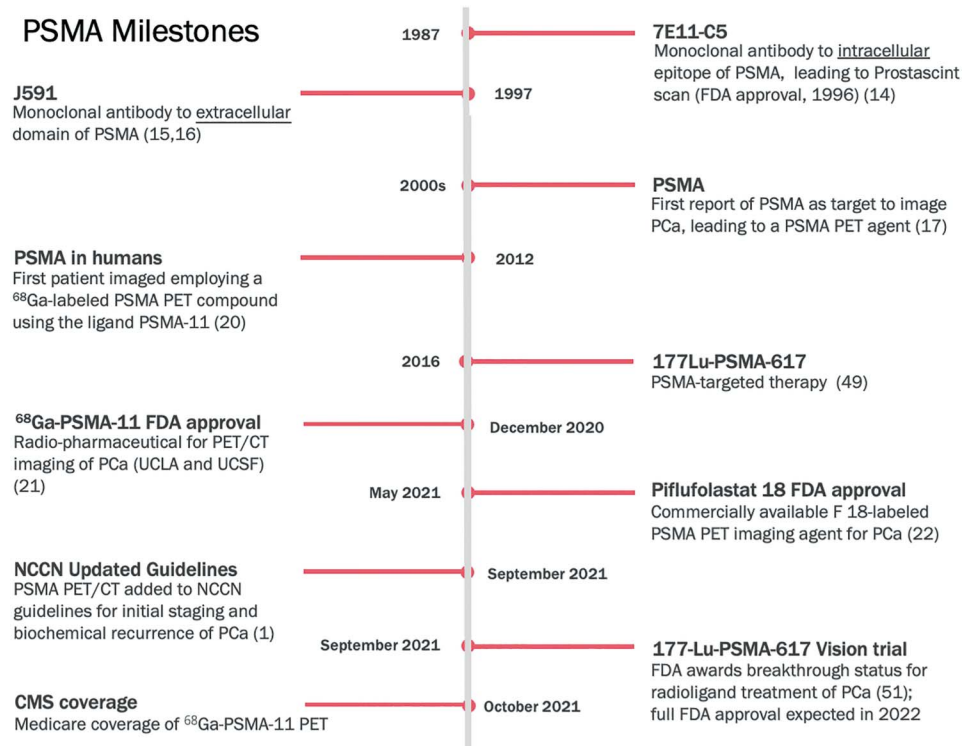


Figure 2. Milestones in development of current PSMA PET/CT scan. CMS, Centers for Medicare and Medicaid Services.

Pivotal PSMA studies used in application to FDA

Indication	Studies	
BCR:		
Author	Fendler et al ²⁸	Morris et al (CONDOR) ³⁹
Yr	2019	2021
No. pts	635	208
Radiotracer	⁶⁸ Ga-PSMA-11	¹⁸ F-DCFPyL
Median age (range)	69 (44–95)	68 (43–91)
Mean ng/ml PSA (range)	2.1 (0.1–1,154)	0.8 (0.2–98.4)
% Sensitivity	90–92	Not available
% Specificity	Not available	Not available
% PPV by histopathology/correlative imaging/PSA response	84/not available/not available	93/89/100
% PPV by composite reference standard	92	Not available
% PPV by region (prostatic/pelvic/extrapelvic)	Not available	80/67/67
% Neg predictive value	Not available	Not available
Inter-reader agreement (Fleiss κ)	0.65–0.78	0.58–0.73
% Whole body detection rate	75	85–87
Pretreatment staging:		
Author	Hope et al ²⁹	Pienta et al (OSPREY) ⁴⁰
Yr	2021	2021
No. pts	277	252
Radiotracer	⁶⁸ Ga-PSMA-11	¹⁸ F-DCFPyL
Median age (range)	69 (63–73)	64 (46–84)
Mean ng/ml PSA (range)	11.1 (6.5–18)	9.7 (1.2–125.3)
% Sensitivity	40	31–42
% Specificity	95	96–99
% PPV	75	78–91
% Neg predictive value	81	81–84
Inter-reader agreement (Fleiss κ)	0.46–0.71	0.71–0.85
% Accuracy of pelvic nodal metastases detection	80	82–84

imaging, which were used in the registration trials for the 2 applications to the FDA, are shown in the table and discussed below.

Examples of PSMA PET/CT scans used for initial staging of PCa and to detect recurrence after treatment are shown in figure 3 (staging) and figure 4 (recurrence). In figure 5, the sensitivity of PSMA PET/CT for detection of metastatic PCa is contrasted with that of CT scanning alone.

GENERAL CHARACTERISTICS OF PSMA SCANS

The following are characteristics that apply universally to PSMA PET/CT scans.

Scan Performance

PET/CT scans are performed in the nuclear medicine department. Radiotracer is administered intravenously. Following tracer uptake (50–100 minutes), PET scanning is performed over the next 20–40 minutes depending on patient size and weight. Fully diagnostic CT is also performed, and the PET/CT images are fused and interpreted. The entire procedure ordinarily takes less than 2 hours including tracer uptake period.²³

Safety Profile

PSMA PET scan includes a radiation dose from the isotope of approximately 4 mSv and an average dose from the CT of 12 mSv. For adults over 50 years of age, the low-dose radiation exposure falls below concerning levels. No serious adverse effects of PSMA scanning have been reported.²⁴

PSMA PET Interpretation

Interpretation for PSMA PET imaging relies on standardized criteria (PROMISE criteria, PSMA-RADS,

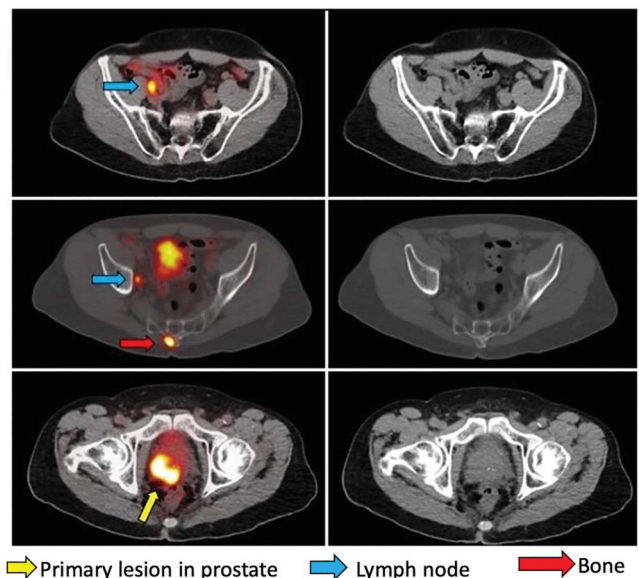


Figure 3. ⁶⁸Ga-PSMA PET/CT scan (left) and corresponding CT scan (right) obtained for primary staging in a 77-year-old patient presenting with PSA of 7.1 ng/ml and prostate biopsy showing Gleason score of 4+5=9. Note clarity of cancerous lesions on PET/CT scan. PSMA expression is seen in the primary tumor (yellow arrow), lymph nodes (blue arrows) and in bone (sacrum, red arrow). NCCN Guidelines for 2021 have included PSMA PET/CT scanning for initial staging and to detect recurrence after primary treatment.¹

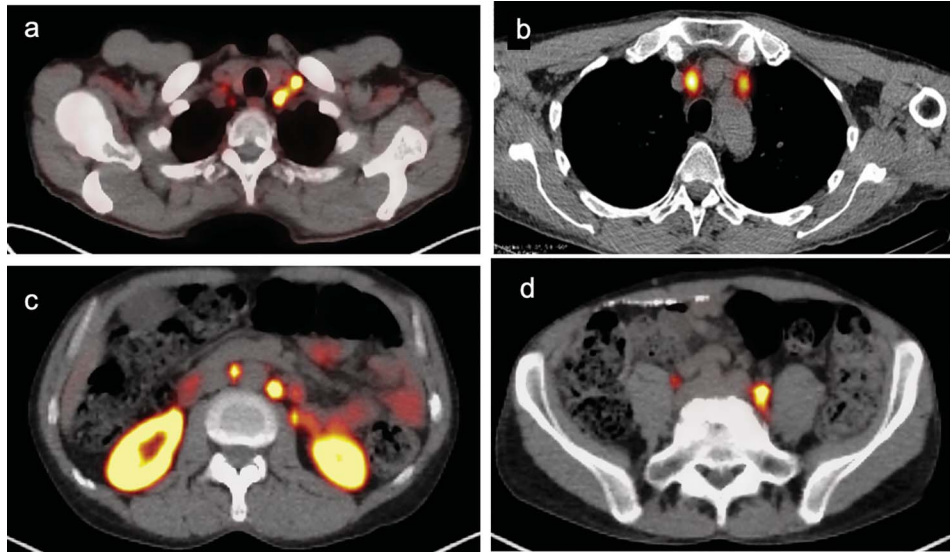


Figure 4. Lymph node metastases. ^{68}Ga -PSMA PET/CT scan obtained for recurrent PCa in a 68-year-old patient with PSA of 24 ng/ml 6 years following radiation therapy for Gleason score 4+4=8 PCa. Note visualization of lymph node metastases in left supraclavicular region (a), mediastinum (b), retroperitoneum (c) and pelvis (d). Radiotracers, which bind to the extracellular epitope of PSMA, allow detection of PCa at various sites throughout the body; lymph node involvement by PCa was often undetectable prior to the advent of PSMA scanning. Uptake of ^{68}Ga in the kidneys (shown here) is physiological.

E-PSMA).^{25–27} The PSMA PET reader follows a “TNM-like” structure. PSMA uptake is analyzed visually and compared to the surrounding background and organs of reference (blood, liver, salivary glands).

Standardized Uptake Value (SUV)

SUV is a metric used to estimate from the PET images the amount of radiotracer in a region. The intensity of PSMA PET signal using SUV can be graded as low (2–4.9), intermediate (5–10) and high (>10). However, SUVs cannot be used as an absolute indicator of PCa. The intensity of PSMA PET signal in a PCa lesion is related to the volume of the lesion and the level of PSMA expression which is correlated with the Gleason score.^{4–7} A high SUV (>10) observed in a location compatible with a PCa lesion on CT is highly specific for PCa. On the other hand, in lesions with low SUVs (2–4.9), there is overlap of PCa and other processes (inflammation, bone trauma, granulomatosis, ganglia, other neoplasms). As for any other PET imaging technique, the visual analysis of the signal-to-background ratio is usually more informative than the absolute intensity of the signal. The SUV represents only 1 parameter among others to make a final diagnosis and should only be used as a complement to the visual analysis.

Inter-reader agreement of interpretation of PSMA PET/CT scans among nuclear medicine physicians is substantial (kappa values 0.6–0.8).^{28,29} This is explained by the very high signal-to-noise ratio observed in PCa lesions, higher than with any other PET imaging technique.³⁰

Reproducibility of PSMA PET signal studies reported that when separate scans were performed some 2 weeks apart, the findings were nearly the same. Within-subject coefficient of variation was 12%–14% for bone and lymph node lesions,³¹ establishing that serial scanning may furnish important clinical information, ie in followup and after treatment.

Performance characteristics of PSMA PET/CT scanning are similar with both FDA-approved scans and are directly related to serum prostate specific antigen (PSA) levels (fig. 6 and text below).

DATA FROM EARLY CLINICAL TRIALS

The peer-reviewed literature on PSMA PET/CT scanning is increasing rapidly, with more than 800 publications listed on PubMed just in the year 2021. Among the first large patient cohorts gathered were those of Afshar-Oromieh³² and Eiber³³ et al in Germany. The value of PSMA PET/CT scanning has been indicated in these and subsequent large, single-arm studies.^{13,34–37} Among the universally-accepted conclusions are that PSMA PET/CT scanning 1) detects PCa lesions—including local recurrences and distant metastases (lymph nodes, bone and viscera)—with greater sensitivity than conventional imaging; 2) demonstrates great specificity for PCa; 3) retains its value during disease progression and androgen deprivation therapy, though with very low serum PSA levels detection rate decreases; 4) identifies intra-prostatic PCa; 5) provides correlation of uptake intensity with PCa disease severity and 6) paves the way for radioligand therapy (RLT) of PCa as a theranostic.

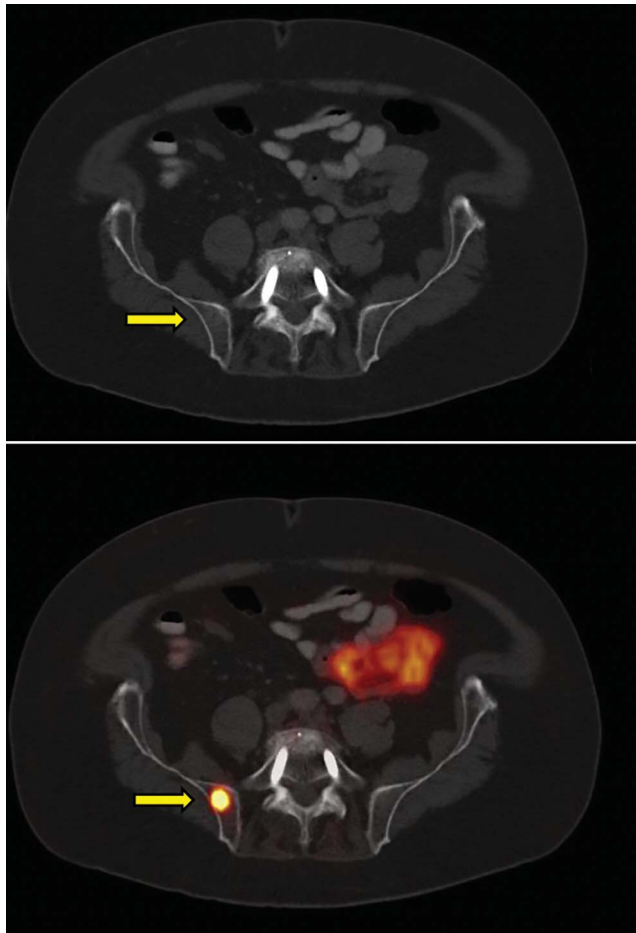


Figure 5. Increased sensitivity of PSMA PET/CT for bony lesion (arrows). CT scan (top) shows no abnormalities, but a lesion of PCa with high PSMA expression (bottom) is apparent in the right ileum. Even in retrospect, the CT scan was unrevealing. Because of the increased sensitivity and specificity, PSMA PET/CT has been added to the NCCN Guidelines for 2021.¹

PATH TO APPROVAL BY FDA

Among the clinical data most thoroughly vetted are the pivotal trials leading to recent FDA approvals (see table). The original trials, upon which the first FDA clearance was based, comprised a unique co-development effort led by imaging specialists at UCSF (Thomas Hope) and UCLA (Johannes Czernin), who were the primary investigators.^{28,29} Fendler reported the UCLA experience with biochemical recurrence (BCR); Hope reported the UCSF experience with pretreatment staging (see table); the imaging agent (⁶⁸Ga-PSMA-11) and the scanning methods were the same at both study sites. For detection of BCR (PSA >0.2 ng/ml), the scan identified the recurrence in 475/635 patients (75%); positive predictive value (PPV) by histopathological validation was 84%.²⁸ For presurgical staging, the scan identified positive pelvic lymph nodes with a sensitivity of 40% and a specificity of 95%, the low sensitivity attributable to undetected micro-metastases.²⁹

Each institution submitted similar Investigational New Drug Applications in late 2016, then matching New Drug Applications in late 2019; ⁶⁸Ga-PSMA-11 was manufactured at each place locally. On December 1, 2020 FDA clearance was received by each institution, marking the first PSMA-targeted PET/CT imaging approvals for PCa. The FDA action cleared ⁶⁸Ga-PSMA-11 for use in PET imaging for men with PCa and (1) suspected metastases who are candidates for initial therapy (2) suspected recurrence based on elevated serum PSA levels. Full details of the path to original FDA approval are available elsewhere.³⁸

FLUORINE-18 PSMA SCAN (PYLARIFY)

A second form of PSMA PET/CT scan, employing the isotope fluorine-18 with the radiotracer ¹⁸F-DCFPyL, entered U.S. clinical trials in 2016 (CONDOR) and 2018 (OSPREY) under sponsorship of Progenics, Inc. (now Lantheus following merger in 2020). Trial results were similar to those in the ⁶⁸Ga-PSMA-11 academic trials above. In the CONDOR trial of BCR (208 patients), detection rate was 59%–66% and PPV was 78%–93%.³⁹ In the OSPREY trial of metastatic/recurrent patients (93), detection rate was 96% (all biopsied) and PPV was 82%; in the OSPREY trial of men with high-risk PCa at initial staging (252), sensitivity for pelvic lymph node detection was 40% (again micro-metastases) and specificity was 98%.⁴⁰ On the basis of these data, FDA clearance was issued to Progenics for ¹⁸F-DCFPyL-PSMA in May 2021 with the same indications as ⁶⁸Ga-PSMA-11. A commercial product is now marketed as Pylarify (pifufolostat F-18).

In figure 6, performance characteristics of the gallium-68 and fluorine-18 based PSMA PET radiotracers are compared in results from separate meta-analyses.^{41,42} While a head-to-head comparison of the 2 radiotracers is not available, detection rates appear similar and are directly related to serum PSA levels. The 2 compounds ¹⁸F-DCFPyL and ⁶⁸Ga-PSMA-11 both target the extracellular domain of PSMA with great affinity, which explains their excellence as imaging agents for PCa. The main difference is the longer half-life of ¹⁸F-DCFPyL (110 minutes) vs that of ⁶⁸Ga-PSMA-11 (68 minutes), which favors supply and distribution of the commercialized product. Kit-based approaches are also available permitting on-site production of the ⁶⁸Ga-labeled compounds.

PSMA VS ¹⁸F-FLUCICLOVINE

The 2 PSMA radio-tracers for PET/CT imaging are not to be confused with the PET imaging agent ¹⁸F-fluciclovine (FACBC, Axumin, Blue Earth Diagnostics, Inc., Burlington, Massachusetts), which lacks affinity for PSMA. ¹⁸F-Fluciclovine is an amino acid analog which detects increased amino acid metabolic activity of cancer. It has been commercially available since FDA approval in 2016. A prospective

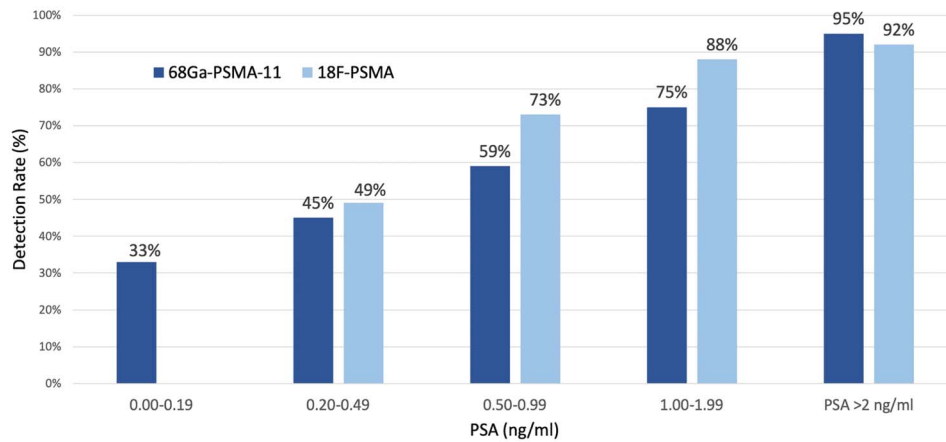


Figure 6. Performance characteristics of 2 FDA-approved versions of PSMA scanning. Dark blue bars represent ^{68}Ga -PSMA (version from UCLA and UCSF) and light blue bars represent ^{18}F -DCFPyL (version commercialized by Lantheus Corp.). Note that cancer detection rates of the 2 PSMA scans are similar and both are directly related to serum PSA levels. Data compiled from meta-analyses.^{41,42}

comparison of ^{18}F -fluciclovine (Axumin) vs ^{68}Ga -PSMA-11 PET/CT in 50 patients with early biochemical recurrent PCa after radical prostatectomy (PSA ≤ 2.0 ng/ml) found ^{68}Ga -PSMA-11 to be a superior imaging modality for overall detection rate of recurrent disease (56% vs 26%).³⁰ ^{68}Ga -PSMA-11 also had a significantly better detection rate for pelvic lymph nodes (30% vs 8%), extra-pelvic nodes (6% vs 0%), bone metastases (8% vs 0%), metastases in other organs (4% vs 0%) and extra-pelvic lesions (16% vs 0%). ^{18}F -fluciclovine was found to have a slightly better detection of lesions in the prostatic bed (18% vs 14%). The lower target-to-background ratio of fluciclovine (up to 8 times lower than for PSMA) is likely to account for differences in diagnostic performance.³⁰ Thus, PSMA appears to be the preferred PET tracer for diagnosis of recurrent PCa.

INTRAPROSTATIC LOCALIZATION OF CANCER

In addition to imaging metastases, PSMA PET/CT scanning may also help localize cancer within the

prostate. Using whole-mount pathology as a reference standard, Donato and colleagues showed an 80% overall concordance for index lesion detection between PSMA PET scans and magnetic resonance imaging (MRI).⁴³ PSMA PET/CT scans detected 13% of tumors missed by MRI; MRI detected 4% of tumors missed by PSMA PET/CT; with the combination, only 2% of index tumors were missed.⁴³ Similar results have been reported in a study employing F-18/PSMA scans.⁴⁴ Using the “gold standard” of whole-mount pathology for correlations, Sonni and colleagues recently showed that the combination of PSMA PET/CT+ multiparametric MRI (mpMRI) provided intraprostatic tumor delineation better than either modality alone.⁴⁵ Thus, pending available technology, PSMA PET/MRI or the fusion of PSMA PET/CT and mpMRI (PSMA PET+mpMRI) deserves further study for localization of primary PCa.

The potential for performing a biopsy, which targets a PSMA-avid spot, was first shown in 2015.⁴⁶ Subsequently, a fusion system was used to sample a PSMA-avid spot (PET/CT-ultrasound), thus diagnosing a

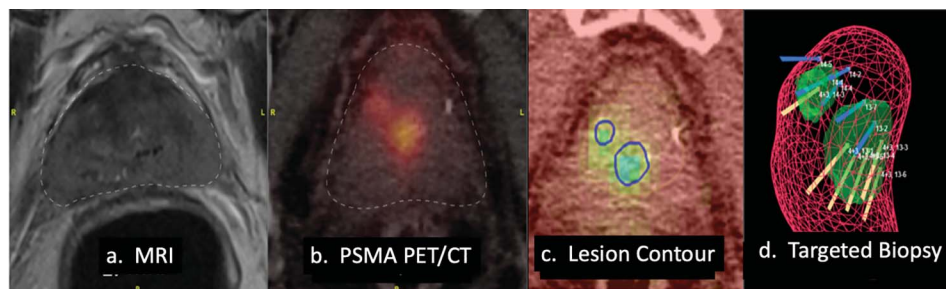


Figure 7. Example of PSMA-guided prostate biopsy in a 71-year-old patient with PSA of 8.5 ng/ml and prostate volume of 25 cc. MRI and systematic biopsy were negative (a). PSMA PET/CT scan shows 2 ^{68}Ga -PSMA-expressing lesions in prostate (b). CT overlay identifies intraprostatic lesions, which are contoured (c). Combining PET/CT with real-time ultrasound allows targeted biopsy using image-fusion device (d).⁴⁷ Biopsies of larger lesion revealed Grade Group 3 PCa.

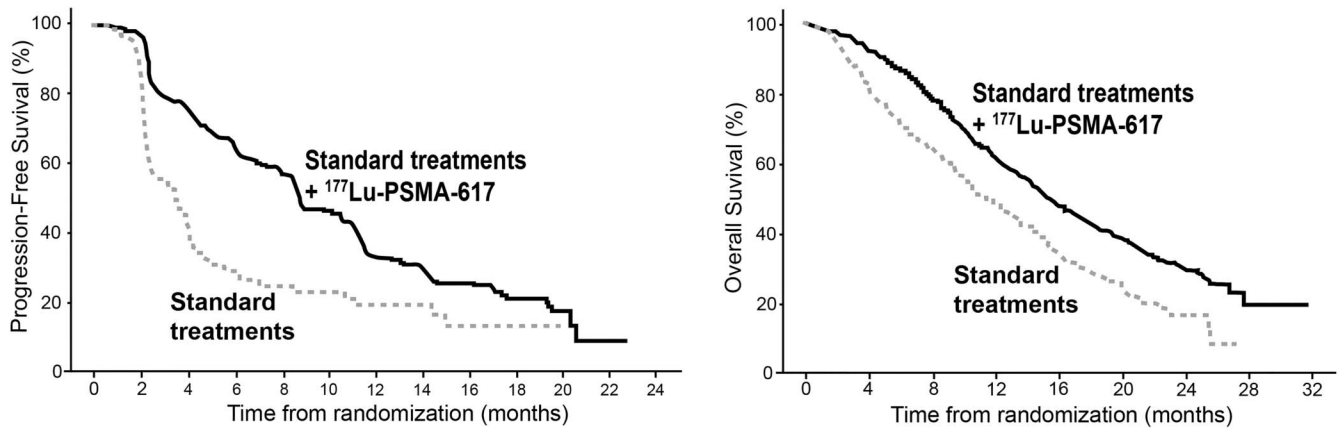


Figure 8. RLT for advanced PCa. Survival curves (A, progression-free; B, overall) show comparison of standard treatments alone (broken lines) and standard treatments with addition of ^{177}Lu -PSMA-617 (solid lines), the radioligand targeting PSMA. Standard treatments included both androgen deprivation and taxanes in all patients. Addition of the radioligand significantly extended progression-free survival and overall survival ($p < 0.001$). Data are reconstructed from Morris et al³⁹ and Sartor et al.⁵¹

serious PCa that could not be detected otherwise.⁴⁷ An example of prostate biopsy successfully detecting an occult PCa by targeting a PSMA-avid lesion is shown in figure 7.

In a large prospective trial (PRIMARY) which compared MRI and PSMA-scanning with biopsy results, Emmett and colleagues found the 2 imaging modalities to provide additive information.³⁵ False-negative rate for clinically significant PCa was 17% with MRI and 10% with PSMA; but only 5/291 men were falsely negative by both, suggesting the

possibility of deferring biopsy in such cases. All men with SUV >12 had clinically significant PCa.³⁵ The value of pre-biopsy imaging, as described in this important paper, deserves further study.

A PSMA-BASED THERANOSTIC

The word “theranostic” is derived from a combination of the words diagnostic and therapeutic, indicating the joint utility of an imaging agent and a therapeutic agent that both target the same receptors. The first theranostic was radioiodine. The gamma-emission of I-131 is detectable by a scanner, and the beta-emission form provides a targeted RLT.⁴⁸ Thus theranostics allow the possibility to treat cancer lesions in a specific and tumor-selective manner.

PSMA-617 is a small molecule that, like PSMA-11, binds with high affinity to the extracellular domain of PSMA. It can be labeled with the beta-emitter lutetium-177 (^{177}Lu) for RLT. The first prospective results of ^{177}Lu -PSMA-617 therapy were reported by Hofman and associates in 2018.⁴⁹ Retrospective analysis of the German compassionate-use program determined that the RLT was effective in patients with metastatic castration-resistant PCa.⁵⁰

Sartor and colleagues confirmed safety and efficacy of ^{177}Lu -PSMA-617 therapy in a large multinational, randomized trial.⁵¹ The landmark VISION trial, which involved 831 men with metastatic castration-resistant PCa, compared standard care alone with standard care plus the RLT in men with metastases visible on ^{68}Ga -PET/CT. Treatment with ^{177}Lu -PSMA-617 was administered every 6 weeks for 4–6 cycles. When lutetium was added to standard care, significant gains were observed in progression-free survival (8.7 vs 3.4 months) and overall survival (15.3 vs 11.3 months; $p < 0.001$). Survival data from the trial are shown in figure 8. Most commonly reported side effects

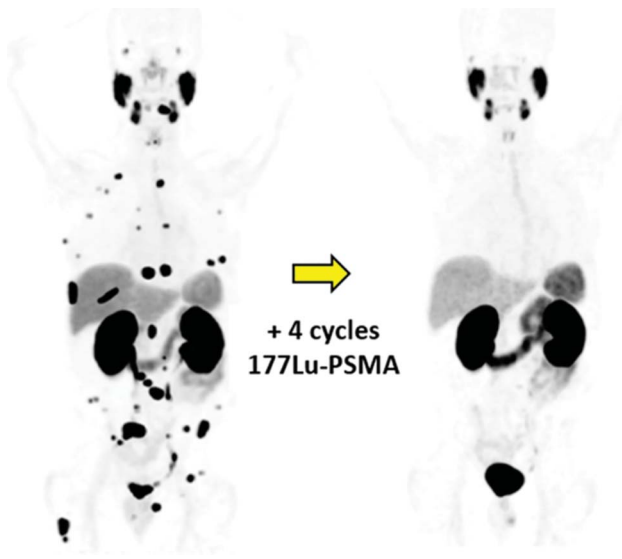


Figure 9. Theranostic application of PSMA PET/CT using ^{177}Lu -PSMA in a 77-year-old patient with castration-resistant, metastatic PCa and PSA of 27 ng/ml (left). After 4 cycles of ^{177}Lu -PSMA over a 63-week period, metastases are no longer apparent (right), and PSA decreased to 0.02 ng/ml. The theranostic is a beta-emitter, which binds to the extracellular epitope of PSMA like the pure imaging agent. At the time of this writing, the PSMA theranostic is under review at FDA.

of lutetium included dry mouth, nausea and fatigue, but overall quality of life was not affected.⁵¹ With these results the sponsor Novartis filed a “new drug application” with the FDA. On September 28, 2021 the agency granted “breakthrough” status for ¹⁷⁷Lu-PSMA-617—a designation reserved for potentially transformative innovations. An example of a dramatic response to ¹⁷⁷Lu-PSMA-617 is shown in figure 9 (patient not from the trial). Approval of the therapeutic is expected in 2022.

THE FUTURE

Assuming real-world experience resembles the clinical trial outcomes, PSMA PET/CT scanning is likely to be widely adopted. A barrier to adoption is availability of the radiotracer. However, according to the manufacturer of Pylarify (Lantheus Medical Imaging, Inc., North Billerica, Massachusetts), as of January 2022 the product is available in the U.S. within a 2-hour drive of 90% of men who might require it (380 facilities, most in metropolitan areas). In the European Union and Australia, the product is available at approximately 150 sites. Another barrier might be availability of PET scanners, but currently some 2,400 PET scanners are in place in the U.S. (versus 12,000 MRI machines). The affordability barrier should come down soon, as Medicare has issued a permanent HCPCS code (Fluor-18, A9595) for the FDA-approved indications (initial staging and biochemical

recurrence), and private payors are expected to follow.

Numerous unmet PCa needs await solutions that may be provided by widespread adoption of PSMA scanning and evaluation in future clinical trials. Improved accuracy of PCa staging is one such need. Use of bone scans and abdominal CT scans would give way to the new imaging procedure, more accurate than the current staging scans. Earlier treatment for recurrent and metastatic disease would be possible, including redefinition of the oligometastatic condition. Some primary cancers, which remain undiagnosed even by MRI, would be found, especially if PET/MRI evolves; earlier curative treatments would be possible. Improved recognition of lesions suitable for partial gland ablation (or not) is another need, which is only partly resolved by current methods. The progression rate of active surveillance might be reduced, if a PSMA scan were negative up-front. For metastatic disease, the armamentarium of treatments would be expanded by therapeutics providing reduced toxicity and improved outcomes compared to what is currently available.

ACKNOWLEDGEMENTS

The current state of PSMA scanning could not have been reached without the key contributions of Thomas Hope, Ken Herrmann, Wolfgang Fendler, Matthias Eiber, Shaojun Zhu, Roger Slavik, Giuseppe Carlucci and Johannes Czernin. Mamdouh N. Aker, MSIII contributed to manuscript research. Figure 1 was created with BioRender.com.

REFERENCES

- Freedman-Cass D, Berardi R, Shead DA et al: NCCN Guidelines Version 1.2022—Prostate Cancer. Plymouth Meeting, Pennsylvania: National Comprehensive Cancer Network 2021. Available at <https://www.nccn.org/home/>.
- Silver DA, Pellicer I, Fair WR et al: Prostate-specific membrane antigen expression in normal and malignant human tissues. *Clin Cancer Res* 1997; **3**: 81.
- Cimadamore A, Cheng M, Santoni M et al: New prostate cancer targets for diagnosis, imaging, and therapy: focus on prostate-specific membrane antigen. *Front Oncol* 2018; **8**: 653.
- Kaittanis C, Andreou C, Hieronymus H et al: Correction: prostate-specific membrane antigen cleavage of vitamin B9 stimulates oncogenic signaling through metabotropic glutamate receptors. *J Exp Med* 2018; **215**: 377.
- Hupe MC, Philippi C, Roth D et al: Expression of prostate-specific membrane antigen (PSMA) on biopsies is an independent risk stratifier of prostate cancer patients at time of initial diagnosis. *Front Oncol* 2018; **8**: 623.
- Ross JS, Sheehan CE, Fisher HA et al: Correlation of primary tumor prostate-specific membrane antigen expression with disease recurrence in prostate cancer. *Clin Cancer Res* 2003; **9**: 6357.
- Perner S, Hofer MD, Kim R et al: Prostate-specific membrane antigen expression as a predictor of prostate cancer progression. *Hum Pathol* 2007; **38**: 696.
- O’Keefe DS, Su SL, Bacich DJ et al: Mapping, genomic organization and promoter analysis of the human prostate-specific membrane antigen gene. *Biochim Biophys Acta* 1998; **1443**: 113.
- Leek J, Lench N, Maraj B et al: Prostate-specific membrane antigen: evidence for the existence of a second related human gene. *Br J Cancer* 1995; **72**: 583.
- Ghosh A and Heston WDW: Tumor target prostate specific membrane antigen (PSMA) and its regulation in prostate cancer. *J Cell Biochem* 2004; **91**: 528.
- Hillier SM, Maresca KP, Femia FJ et al: Preclinical evaluation of novel glutamate-urea-lysine analogues that target prostate-specific membrane antigen as molecular imaging pharmaceuticals for prostate cancer. *Cancer Res* 2009; **69**: 6932.
- Mhaweche-Fauceglia P, Zhang S, Terracciano L et al: Prostate-specific membrane antigen (PSMA) protein expression in normal and neoplastic tissues and its sensitivity and specificity in prostate adenocarcinoma: an immunohistochemical study using multiple tumour tissue microarray technique. *Histopathology* 2007; **50**: 472.
- Maurer T, Eiber M, Schwaiger M et al: Current use of PSMA-PET in prostate cancer management. *Nat Rev Urol* 2016; **13**: 226.
- Horoszewicz JS, Kawinski E and Murphy GP: Monoclonal antibodies to a new antigenic marker in epithelial prostatic cells and serum of prostatic cancer patients. *Anticancer Res* 1987; **7**: 927.
- Smith-Jones PM, Vallabhajosula S, Goldsmith SJ et al: Vitro characterization of radiolabeled monoclonal antibodies specific for the

- extracellular domain of prostate-specific membrane antigen. *Cancer Res* 2000; **60**: 5237.
16. Tagawa ST, Vallabhajosula S, Christos PJ et al: Phase 1/2 study of fractionated dose lutetium-177-labeled anti-prostate-specific membrane antigen monoclonal antibody J591 (¹⁷⁷Lu-J591) for metastatic castration-resistant prostate cancer. *Cancer* 2019; **125**: 2561.
 17. Foss CA, Mease RC, Fan H et al: Radiolabeled small-molecule ligands for prostate-specific membrane antigen: in vivo imaging in experimental models of prostate cancer. *Clin Cancer Res* 2005; **11**: 4022.
 18. Choyke PL and Bouchelouche K: Prostate specific membrane antigen (PSMA) imaging: the past is prologue. *Translational Androl Urol* 2019; **8**: 283.
 19. Rowe SP, Gorin MA and Pomper MG: Imaging of prostate-specific membrane antigen with small-molecule PET radiotracers: from the bench to advanced clinical applications. *Annu Rev Med* 2019; **70**: 461.
 20. Eder M, Schäfer M, Bauder-Wüst U et al: ⁶⁸Ga-complex lipophilicity and the targeting property of a urea-based PSMA inhibitor for PET imaging. *Bioconjug Chem* 2012; **23**: 688.
 21. The FDA approves PSMA targeted drug for PET imaging in men with prostate cancer. *BJU Int* 2021; **127**: 267.
 22. U.S. Food and Drug Administration: FDA approves second PSMA-targeted PET imaging drug for men with prostate cancer. Available at <https://www.fda.gov/drugs/news-events-human-drugs/fda-approves-second-psma-targeted-pet-imaging-drug-men-prostate-cancer>.
 23. Fendler WP, Eiber M, Beheshti M et al: ⁶⁸Ga-PSMA PET/CT: joint EANM and SNMMI procedure guideline for prostate cancer imaging: version 1.0. *Eur J Nucl Med Mol Imaging* 2017; **44**: 1014.
 24. Jadvar H, Calais J, Fanti S et al: Appropriate use criteria for prostate-specific membrane antigen PET imaging. *J Nucl Med* 2022; **63**: 59.
 25. Eiber M, Herrmann K, Calais J et al: Prostate cancer molecular imaging standardized evaluation (PROMISE): proposed mITNM classification for the interpretation of PSMA-ligand PET/CT. *J Nucl Med* 2018; **59**: 469.
 26. Rowe SP, Pienta KJ, Pomper MG et al: PSMA-RADS version 1.0: a step towards standardizing the interpretation and reporting of PSMA-targeted PET imaging studies. *Eur Urol* 2018; **73**: 485.
 27. Ceci F, Oprea-Lager DE, Emmett L et al: E-PSMA: the EANM standardized reporting guidelines v1.0 for PSMA-PET. *Eur J Nucl Med Mol Imaging* 2021; **48**: 1626.
 28. Fendler WP, Calais J, Eiber M et al: Assessment of ⁶⁸Ga-PSMA-11 PET accuracy in localizing recurrent prostate cancer: a prospective single-arm clinical trial. *JAMA Oncol* 2019; **5**: 856.
 29. Hope TA, Eiber M, Armstrong WR et al: Diagnostic accuracy of ⁶⁸Ga-PSMA-11 PET for pelvic nodal metastasis detection prior to radical prostatectomy and pelvic lymph node dissection: a multicenter prospective phase 3 imaging trial. *JAMA Oncol* 2021; **7**: 1635.
 30. Calais J, Ceci F, Eiber M et al: ¹⁸F-fluciclovine PET-CT and ⁶⁸Ga-PSMA-11 PET-CT in patients with early biochemical recurrence after prostatectomy: a prospective, single-centre, single-arm, comparative imaging trial. *Lancet Oncol* 2019; **20**: 1286.
 31. Pollard JH, Raman C, Zakharia Y et al: Quantitative test-retest measurement of ⁶⁸Ga-PSMA-HBED-CC in tumor and normal tissue. *J Nucl Med* 2020; **61**: 1145.
 32. Afshar-Oromieh A, Avtzi E, Giesel FL et al: The diagnostic value of PET/CT imaging with the ⁶⁸Ga-labelled PSMA ligand HBED-CC in the diagnosis of recurrent prostate cancer. *Eur J Nucl Med Mol Imaging* 2015; **42**: 197.
 33. Eiber M, Maurer T, Souvatzoglou M et al: Evaluation of hybrid ⁶⁸Ga-PSMA ligand PET/CT in 248 patients with biochemical recurrence after radical prostatectomy. *J Nucl Med* 2015; **56**: 668.
 34. Hofman MS, Lawrentschuk N, Francis RJ et al: Prostate-specific membrane antigen PET-CT in patients with high-risk prostate cancer before curative-intent surgery or radiotherapy (proPSMA): a prospective, randomised, multicentre study. *Lancet* 2020; **395**: 1208.
 35. Emmett L, Buteau J, Papa N et al: The additive diagnostic value of prostate-specific membrane antigen positron emission tomography computed tomography to multiparametric magnetic resonance imaging triage in the diagnosis of prostate cancer (PRIMARY): a prospective multicentre study. *Eur Urol* 2021; **80**: 682.
 36. Roach PJ, Francis R, Emmett L et al: The impact of ⁶⁸Ga-PSMA PET/CT on management intent in prostate cancer: results of an Australian prospective multicenter study. *J Nucl Med* 2018; **59**: 82.
 37. Keidar Z, Gill R, Goshen E et al: ⁶⁸Ga-PSMA PET/CT in prostate cancer patients—patterns of disease, benign findings and pitfalls. *Cancer Imaging* 2018; **18**: 39.
 38. Carlucci G, Ippisch R, Slavik R et al: ⁶⁸Ga-PSMA-11 NDA approval: a novel and successful academic partnership. *J Nucl Med* 2021; **62**: 149.
 39. Morris MJ, Rowe SP, Gorin MA et al: Diagnostic performance of ¹⁸F-DCFPyL-PET/CT in men with biochemically recurrent prostate cancer: results from the CONDOR phase III, multicenter study. *Clin Cancer Res* 2021; **27**: 3674.
 40. Pienta KJ, Gorin MA, Rowe SP et al: A phase 2/3 prospective multicenter study of the diagnostic accuracy of prostate specific membrane antigen PET/CT with ¹⁸F-DCFPyL in prostate cancer patients (OSPReY). *J Urol* 2021; **206**: 52.
 41. Perera M, Papa N, Roberts M et al: Gallium-68 prostate-specific membrane antigen positron emission tomography in advanced prostate cancer—updated diagnostic utility, sensitivity, specificity, and distribution of prostate-specific membrane antigen-avid lesions: a systematic review and meta-analysis. *Eur Urol* 2020; **77**: 403.
 42. Treglia G, Annunziata S, Pizzuto DA et al: Detection rate of ¹⁸F-labeled PSMA PET/CT in biochemical recurrent prostate cancer: a systematic review and a meta-analysis. *Cancers* 2019; **11**: 710.
 43. Donato P, Morton A, Yaxley J et al: ⁶⁸Ga-PSMA PET/CT better characterises localised prostate cancer after MRI and transperineal prostate biopsy: is ⁶⁸Ga-PSMA PET/CT guided biopsy the future? *Eur J Nucl Med Mol Imaging* 2020; **47**: 1843.
 44. Bodar YJL, Jansen BHE, van der Voorn JP et al: Detection of prostate cancer with ¹⁸F-DCFPyL PET/CT compared to final histopathology of radical prostatectomy specimens: is PSMA-targeted biopsy feasible? The DeTeCT trial. *World J Urol* 2021; **39**: 2439.
 45. Sonni I, Felker ER, Lenis AT et al: Head-to-head comparison of ⁶⁸Ga-PSMA-11 PET/CT and mpMRI with histopathology gold-standard in the detection, intra-prostatic localization and local extension of primary prostate cancer: results from a prospective single-center imaging trial. *J Nucl Med* 2021; <https://doi.org/10.2967/jnumed.121.262398>.
 46. Zettinig O, Shah A, Hennersperger C et al: Multimodal image-guided prostate fusion biopsy based on automatic deformable registration. *Int J Comput Assist Radiol Surg* 2015; **10**: 1997.
 47. Simopoulos DN, Natarajan S, Jones TA et al: Targeted prostate biopsy using ⁶⁸Gallium PSMA-PET/CT for image guidance. *Urol Case Rep* 2017; **14**: 11.
 48. Inubushi M, Miura H, Kuji I et al: Current status of radioligand therapy and positron-emission tomography with prostate-specific membrane antigen. *Ann Nucl Med* 2020; **34**: 879.
 49. Hofman MS, Violet J, Hicks RJ et al: [¹⁷⁷Lu]-PSMA-617 radionuclide treatment in patients with metastatic castration-resistant prostate cancer (LuPSMA trial): a single-centre, single-arm, phase 2 study. *Lancet Oncol* 2018; **19**: 825.
 50. Rahbar K, Ahmadzadehfard H, Kratochwil C et al: German multicenter study investigating ¹⁷⁷Lu-PSMA-617 radioligand therapy in advanced prostate cancer patients. *J Nucl Med* 2017; **58**: 85.
 51. Sartor O, de Bono J, Chi KN et al: Lutetium-177-PSMA-617 for metastatic castration-resistant prostate cancer. *N Engl J Med* 2021; **385**: 1091.

Testicular Cancer

JU Insight

Accuracy of 18F-Fluorodeoxyglucose Positron Emission Tomography in Early Metastatic Testicular Seminoma: Analysis From the SEMS Trial

Brian Hu, Muhannad Alsyouf, Ala'a Farkouh, et al.

Correspondence: Brian Hu (bhu@llu.edu).

Full-length article available at <https://doi.org/10.1097/JU.0000000000004561>.

Study Need and Importance: Positron emission tomography (PET) scans are not recommended for the primary staging of testicular germ cell tumors, although PET is commonly used in practice. Its utility has been hampered by rates of false-positive scans and a paucity of data on its true accuracy. A new frontier in testicular cancer—primary surgical treatment in seminoma with retroperitoneal lymphadenopathy—allows a window into the accuracy of PET scans. The SEMS (Surgery in Early Metastatic Seminoma) trial prospectively evaluated retroperitoneal lymph node dissection to treat testicular seminoma with limited retroperitoneal adenopathy and included a PET radiographic correlate.

What We Found: From the 55 patients enrolled in the trial, PET scans were performed in 26 patients and compared with surgical pathology at the time of retroperitoneal lymph node dissection. PET performed favorably in the ability to predict positive and negative retroperitoneal lymph nodes when compared with pathology specimens. The Figure presents the accuracy of PET stratified by radiographic and pathologic positivity. There were no extraretroperitoneal PET findings that represented seminoma on follow-up.

Limitations: The study evaluated PET accuracy in isolation, although the actual value of a study is in

	Pathologic Node +	Pathologic Node -	
PET +	18	2	PPV 90%
PET -	1	5	NPV 83%
	Sensitivity 95%		Specificity 71%

Figure. Diagnostic accuracy of 18F-fluorodeoxyglucose positron emission tomography (PET) in identifying metastatic seminoma compared with pathologic confirmation. NPV indicates negative predictive value; PPV, positive predictive value.

its ability to improve disease detection beyond currently clinical, radiographic, and pathologic factors. All patients in the SEMS study were treated at tertiary care facilities with multidisciplinary teams and high pretest probability of positive retroperitoneal disease; thus, the added benefit of the PET scan in clinical assessment was limited.

Interpretation for Patient Care: Despite the accuracy of in patients with early clinical stage IIA-B seminoma, the use of PET scan to evaluate for cancer is not recommended. More robust evaluation of PET scanning is required before integrating this study into clinical staging.

Accuracy of 18F-Fluorodeoxyglucose Positron Emission Tomography in Early Metastatic Testicular Seminoma: Analysis From the SEMS Trial

Brian Hu,¹ Muhannad Alsyof,¹ Ala'a Farkouh,¹ Clint Cary,² Timothy Masterson,² Lawrence Einhorn,³ Nabil Adra,³ Stephen A. Boorjian,⁴ Christian Kollmannsberger,⁵ Anne Schuckman,⁶ Alan So,⁷ Peter C. Black,⁷ Aditya Bagrodia,⁸ Eila Skinner,⁹ Mehrdad Alemozaffar,¹⁰ Timothy Brand,¹¹ Scott Eggener,¹² Phillip Pierorazio,¹³ Kelly Stratton,¹⁴ Lucia Nappi,^{5,7} Craig Nichols,¹⁵ and Siamak Daneshmand⁶

¹Department of Urology, Loma Linda University Health, Loma Linda, California

²Department of Urology, Indiana University School of Medicine, Indianapolis, Indiana

³Division of Hematology-Oncology, Indiana University Simon Comprehensive Cancer Center, Indianapolis, Indiana

⁴Department of Urology, Mayo Clinic, Rochester, Minnesota

⁵Division of Medical Oncology, British Columbia Cancer-Vancouver Cancer Centre, Vancouver, British Columbia, Canada

⁶Department of Urology, USC/Norris Comprehensive Cancer Center, Los Angeles, California

⁷Department of Urologic Sciences, University of British Columbia, Vancouver Prostate Centre, Vancouver, British Columbia, Canada

⁸Department of Urology, University of California San Diego, La Jolla, California

⁹Department of Urology, Stanford University, Stanford, California

¹⁰Department of Urology, Kaiser Permanente, Los Angeles, California

¹¹Department of Urology, Madigan Army Medical Center, Tacoma, Washington

¹²Section of Urology, Department of Surgery, University of Chicago Medical Center, Chicago, Illinois

¹³Department of Surgery, Division of Urology, University of Pennsylvania, Philadelphia, Pennsylvania

¹⁴Department of Urology, University of Oklahoma Health Sciences Center, Oklahoma City, Oklahoma

¹⁵Testicular Cancer Commons, Portland, Oregon

Purpose: Recent clinical trials on primary retroperitoneal lymph node dissection (RPLND) for testicular seminoma highlight inaccuracies in conventional imaging for lymph node staging. Limited data exist on the accuracy of

Submitted February 3, 2025; accepted April 2, 2025; published April 9, 2025.

Recusal: Dr Bagrodia and Dr Daneshmand are on the editorial board of *The Journal of Urology*® and were recused from the editorial and peer review processes. Dr Eggener is an associate editor of *The Journal of Urology*® and was recused from the editorial and peer review processes. Dr Pierorazio is an AUA publications online content editor and was recused from the editorial and peer review processes.

Funding/Support: None.

Conflict of Interest Disclosures: Dr Black reported being an advisor for AbbVie, Astellas, AstraZeneca, Aura, Bayer, BMS, CG Oncology, Combat, EMD-Serono, EnGene, Ferring, Janssen, Merck, Nonagen, Nanology, Nanobot, Pfizer, Photocure, Prokarium, Sumitomo, TerSera, Tolmar, and Verity; a speaker for Janssen, TerSera, Bayer, and Pfizer; and a clinical trials investigator for Janssen, CG Oncology, EnGene, Verity, Therelase, Pacific Edge, and Pfizer. Dr Boorjian reported having a financial interest/and or other relationship with Ferring, ArTara, and Prokarium, and reported being a consultant for Johnson and Johnson. Dr Pierorazio reported being a board member of the Testicular Cancer Awareness Foundation. No other disclosures were reported.

Ethics Statement: This study received Institutional Review Board approval (IRB No. NCT02537548).

Author Contributions:

Conception and design: Schuckman, Hu, Cary, Skinner, Black, Daneshmand, Brand, Masterson.

Data analysis and interpretation: Bagrodia, Farkouh, Hu, Kollmannsberger, Cary, Nichols, Skinner, Stratton, Nappi, Alsyof, Adra, Black, Daneshmand, Boorjian, Brand, Masterson.

Data acquisition: Bagrodia, So, Schuckman, Hu, Kollmannsberger, Skinner, Einhorn, Alemozaffar, Adra, Black, Eggener, Pierorazio, Daneshmand, Brand, Masterson.

Critical revision of the manuscript for scientific and factual content: Bagrodia, Farkouh, So, Schuckman, Hu, Kollmannsberger, Cary, Nichols, Skinner, Stratton, Einhorn, Nappi, Alemozaffar, Adra, Black, Eggener, Pierorazio, Daneshmand, Boorjian, Brand, Masterson.

Drafting the manuscript: Farkouh, Schuckman, Hu, Kollmannsberger, Alsyof, Daneshmand, Brand, Masterson.

Statistical analysis: Farkouh, Hu, Alsyof, Brand.

Supervision: Bagrodia, So, Schuckman, Hu, Kollmannsberger, Cary, Nichols, Skinner, Stratton, Einhorn, Alemozaffar, Adra, Black, Eggener, Pierorazio, Daneshmand, Boorjian, Brand, Masterson.

Patient selection and data: Schuckman, Hu, Alsyof, Daneshmand.

Review and revisions: Kollmannsberger, Hu, Alsyof, Daneshmand.

Data interpretation: Nappi, Hu, Alsyof, Daneshmand.

Corresponding Author: Brian Hu, MD, Department of Urology, Loma Linda University Health, 11234 Anderson St, Room A560, Loma Linda, CA 92354 (bhu@llu.edu).

positron emission tomography (PET) in patients with chemotherapy-naïve testicular seminoma. We evaluated the accuracy of 18F-fluorodeoxyglucose (FDG) PET for the detection of metastatic disease within the SEMS (Surgery in Early Metastatic Seminoma) trial.

Materials and Methods: The SEMS trial is a phase 2 prospective study evaluating efficacy of primary RPLND in patients with testicular seminoma with limited retroperitoneal lymphadenopathy. 18F-FDG PET scanning was performed as a radiographic correlate in addition to standard axial imaging before surgery. PET findings were based on local interpretation, and the results were compared with surgical pathology.

Results: Of the 55 patients enrolled in the trial, 26 (47%) underwent PET. Twenty (77%) scans were reported as positive with lymph nodes in the retroperitoneum, pelvis, or inguinal region. Of the positive PET scans, 18 had pathologically positive lymph nodes (positive predictive value 90%) at the time of RPLND. Six PET scans were negative with 5 of these patients having surgically confirmed pN0 disease (negative predictive value 83%). Sensitivity of PET for detecting lymph node metastatic seminoma was 95% and specificity was 71%. The average standardized uptake values of the PET-positive lymph nodes and pathologically positive lymph nodes were 7.0 (range 2.6-18.8) and 6.8 (range 1.53-18.8), respectively. No PET-positive lesions outside of the retroperitoneum or pelvis were found to represent metastatic seminoma on clinical follow-up.

Conclusions: In patients with testicular seminoma, 18F-FDG PET findings correlated with both pathologically positive and negative retroperitoneal lymph nodes in most cases. Further research is needed to determine if PET can improve on the already good predictive performance of conventional imaging and clinical expertise.

Key Words: seminoma, positron-emission tomography, diagnosis, neoplasm staging, predictive value of tests

With advances in the management of testicular cancer, survival outcomes are excellent, but patients can be burdened with long-term morbidity.^{1,2} These morbidities are often treatment-related, and efforts at improving testis cancer survivorship by avoiding unnecessary treatment or testing remain an area of emphasis. Improving the accuracy of staging could yield significant benefits for patients with testicular cancer as current staging modalities have limitations. Surgical studies of primary retroperitoneal lymph node dissection (RPLND) for stage II germ cell tumors have found that pN0 rates are as high as 22% for seminoma and 53% for nonseminomatous germ cell tumors depending on selection criteria for surgery.^{3,4} Among patients with stage I germ cell tumors, up to 30% will develop metastases that potentially could have been detected earlier with more sensitive imaging or blood-based markers.⁵ Refinement in the accuracy of clinical staging could lead to equivalent excellent therapeutic outcomes with a reduced patient burden.

18F-fluorodeoxyglucose (FDG) positron emission tomography (PET) is sometimes used in the management of metastatic seminoma to assess residual postchemotherapy masses, although operating characteristics are poor and robust evidence of clinical utility is lacking.¹ In the more common setting of initial staging in either seminoma or nonseminoma, PET scan is not recommended and is hampered by high false-positive and false-negative findings. Despite this, PET scanning as an initial staging modality is performed at some centers.

The Surgery in Early Metastatic Seminoma (SEMS) study is a North American, multi-institutional single-arm prospective phase 2 clinical trial.⁶ Twelve sites were qualified before beginning enrollment through review of institutional surgical volumes of open RPLND and intraoperative photography. It evaluated the efficacy of primary RPLND to treat patients with testicular seminoma and enlarged retroperitoneal lymph nodes (1-3 cm). As a secondary objective, the trial provided a unique opportunity for evaluation into the accuracy of PET for staging. Patients were prospectively enrolled, and all underwent RPLND with resultant surgical pathology. In this study, we report the diagnostic accuracy of 18F-FDG PET imaging in testicular seminoma through pathological assessment of specimens obtained in the setting of therapeutic primary RPLND as well as through clinical follow-up for recurrence.

METHODS

In the SEMS trial, the decision for inclusion and assessment of lymphadenopathy was based on conventional abdomen/pelvis axial imaging performed in high-volume, surgical centers of excellence. Before RPLND, 18F-FDG PET was performed as an optional radiographic correlate to enrollment. The PET was performed at the discretion of the site investigator, and scans were performed and interpreted at the tertiary care institution. Patients were then treated with open RPLND by qualified urologic oncologists with lymph nodes being sent for pathologic review in packets according to anatomic location.

Lymph node size, lymph node number, location of positive lymph node, maximal standardized uptake value

(SUV), and other incidental findings on PET were reviewed. The interpretation of PET scan positivity was based on radiologic interpretation from each of the 12 high-volume germ cell tumor centers. The PET findings were compared with the RPLND pathology report and clinical follow-up. Descriptive results were synthesized, and the sensitivity, specificity, positive predictive value (PPV), and negative predictive value (NPV) of PET scans were calculated. Associations between PET positivity and serum tumor markers status or time between orchiectomy and RPLND were evaluated with the Fisher exact test and the Mann-Whitney *U* test, respectively.

RESULTS

Of the 55 patients enrolled in the SEMS trial, 26/55 (47%) had a PET scan performed at an average of 22 days (range 1-90) before surgery. Twelve SEMS sites had at least 1 patient included in this study. Twenty of the 26 patients with PET scans (77%) were reported as positive with disease limited to lymph nodes in the retroperitoneum, pelvis, or inguinal region. A solitary lymph node was reported as positive in 14/20 patients (70%), while 6 patients had > 1 positive lymph node. Figure 1 shows a representative CT scan with an enlarged retroperitoneal lymph node and corresponding PET scan with a solitary positive lymph node uptake. The average SUV of a positive lymph node on PET was 7.0 (range 2.6-18.8). The average SUV of pathologically positive lymph nodes was 6.82 (range 1.53-18.8).

When compared with surgical pathology, 18 of the 20 positive PET scans were confirmed to be true positives for retroperitoneal spread of seminoma, yielding a PPV of 90%. The size of the metastatic deposits was variable with a median size of 2.1 cm (range 0.3 mm-6 cm). Of the 6 patients with negative PET scans, one was found to have a metastatic

retroperitoneal lymph node on pathology, yielding a NPV of 83%. None of the patients with negative PET scan and pN0 disease experienced a recurrence of seminoma (median follow-up 37 months). Sensitivity of PET in detecting retroperitoneal spread of seminoma was 95% and specificity was 71%. Figure 2 is a 2 × 2 contingency table demonstrating the sensitivity, specificity, PPV, and NPV of 18F-FDG PET in identifying metastatic seminoma to the retroperitoneum. Patients who had a negative PET scan were more likely to have negative serum tumor markers when compared with those who had a positive PET (83% vs 65%, *P* = .63). The timing of retroperitoneal lymphadenopathy was shorter in patients who had a negative PET, although this was also not statistically significant (median 2.5 months vs 8.2 months, *P* = .14).

Radiographic findings outside of the retroperitoneal and pelvic lymph nodes were notable in several patients. One patient had 3 ipsilateral inguinal lymph nodes 8 to 10 mm in size that had SUVs ranging from 1.5 to 2.1. This was in addition to having multiple lymph nodes in the paraaortic and external iliac region between 7 and 10 mm with SUV from 1.3 to 4.0. The patient's PET was reported as positive for metastatic seminoma, although the patient had no cancer at time of RPLND, did not undergo an inguinal lymphadenectomy, and did not experience disease recurrence during follow-up. Another patient had a 3.1-cm lung lesion with air bronchograms and SUV max of 10.3. This was interpreted as either infectious or neoplastic and depending on clinical correlation. Given no clear interpretation in favor of cancer, the chest finding was categorized as negative. Five scans (19%) reported on incidental findings, and most of these were cervical lymph node or tonsillar uptake, not suspicious for metastasis. None of the 7 patients

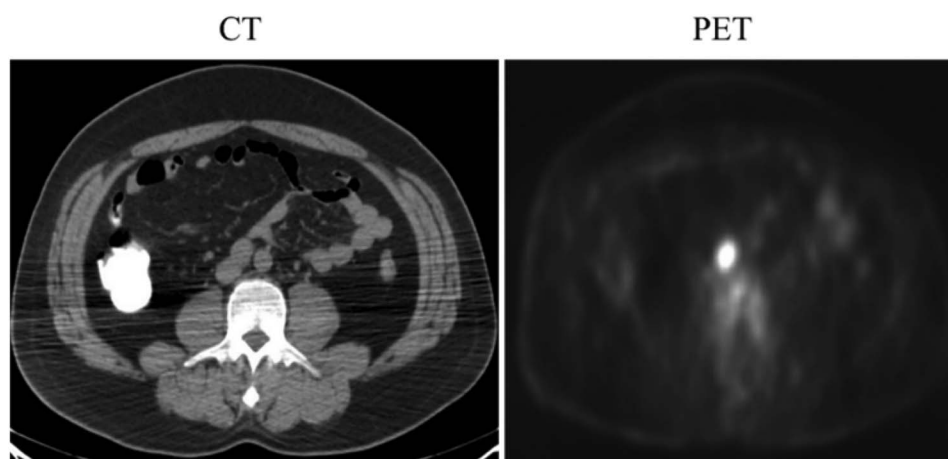


Figure 1. CT scan showing a single enlarged retroperitoneal lymph node in a patient with seminoma and corresponding positron emission tomography (PET) scan showing enhancement. Surgical pathology was consistent with metastatic seminoma.

	Pathologic Node +	Pathologic Node -	
PET +	18	2	PPV 90%
PET -	1	5	NPV 83%
	Sensitivity 95%	Specificity 71%	

Figure 2. Diagnostic accuracy of 18F-fluorodeoxyglucose positron emission tomography (PET) in identifying metastatic seminoma compared with pathologic confirmation. NPV indicates negative predictive value; PPV, positive predictive value.

with findings outside of the abdomen or pelvis were found to have extraretroperitoneal testicular seminoma on follow-up (median 27 months).

Three scans were discordant from final pathology. One patient had a 1-cm left internal iliac lymph node with mild reactivity (SUV 4.2) that favored a metastatic lymph node, but interpretation was confounded by potential avidity from the adjacent ureter. The second patient was previously discussed with multiple small retroperitoneal, pelvic, and inguinal lymph nodes with mild avidity SUV (range 1.5-2.6) that was interpreted as positive for metastatic seminoma. The third patient with a 0.8-cm retroperitoneal lymph node with a maximum SUV of 1.53, which was less than liver activity and interpreted as negative. At the time of RPLND, he was found 2 metastatic lymph nodes, the largest with a 1.1-cm metastatic deposit with extranodal extension. The PET was performed 41 days before RPLND which was longer than the mean for the entire cohort (22 days). The 5 true negative studies were performed on average 10 days before RPLND (range 2-23 days).

When correlating the PET findings to pathologic findings, PET scan accurately identified the number of positive lymph nodes only 50% of the time. As pathology typically reported the size of the largest lymph node, not all positive lymph node sizes were known. When reported, the size of the missed metastatic lymph nodes ranged from 0.7 mm to 1 cm. Reported anatomic sites of lymph node involvement on PET scans were correct in 16 of 19 patients (84%) when compared with locations of metastatic nodes in the resected surgical specimens.

DISCUSSION

Our study revealed that PET findings correlated well with retroperitoneal surgical pathology in testicular seminoma in a prospective clinical trial. This noninvasive, readily available imaging had operating

characteristics comparable with standard and more broadly available clinical decision-making tools available at expert centers with a PPV of 90% and NPV of 83%. In this study population with isolated clinically positive retroperitoneal lymph nodes, a PET scan performed in parallel did not detect an instance of extraretroperitoneal metastatic disease on clinical follow-up. PET was also not accurate in predicting the number of positive retroperitoneal lymph nodes. There are several potential reasons for this but most likely related to adjacent nodes being interpreted as a single lymph node, small volume non-FDG avid metastasis, or potentially artifact from surgical excision and pathological processing.

While the accuracy of PET within our study was good, it should not be interpreted as an endorsement of PET in the primary setting. The true impact of a study lies in its ability to augment staging beyond current clinical, radiographic, and pathological variables. The accuracy of PET within this study overlaps with the operating characteristics of clinical staging with conventional imaging and clinical expertise.^{3,7} Importantly, the patients enrolled in SEMS were diagnosed and treated at highly selected centers with rigorous multidisciplinary teams and with a high pre-PET scan probability of disease. Other groups have studied PET in the primary setting and found good PPV, fair NPV, and noted that the PET results that had minimal to no impact on clinical decision making.^{8,9} Confounding by inflammatory processes and poor performance in low volume disease (<5 mm) represent obstacles to its adoption and a reason why PET for primary staging is not recommended.^{1,10-12}

Closer evaluation of the discordance between PET and surgical pathology helps to understand the weaknesses of the study and the potentially the biology of metastatic seminoma. Within this radiographic correlate with SEMS, there were 2 false-positive studies and 1 false-negative study with reasons potentially related to the test itself, the

interpretation, or metastatic seminoma occurring between the time of the test and surgery. One patient with a false-positive study had multiple inguinal, pelvic, and retroperitoneal lymph nodes with mild uptake (SUV 1.5-2.6) that were interpreted as metastatic. There is no clear cutoff for a positive lymph node with respect to SUV, and indeed, this study identified a pathologically positive lymph node with SUV as low as 1.53. In a PET with mild reactivity, interobserver variability is higher and reliance on knowledge of the natural history of metastatic seminoma becomes emphasized. With the benefit of hindsight, the PET with diffuse mild uptake in lymph nodes including the inguinal region should have favored an inflammatory of physiologic etiology over cancer. The other false-positive PET in this study identified a lesion that was interpreted as a metastatic lymph node over an adjacent ureter. This case provides an excellent example of the nuances in clinical staging and how difficult it can be to determine the utility of one study, in isolation. A radiographic interpretation from one study is insufficient, and clinical staging should be performed with multidisciplinary input evaluating all clinical, pathologic, and radiographic factors. Finally, the false-negative study may not have been due to inaccuracy of PET. The false-negative study was conducted 41 days before RPLND which was longer than the mean for the entire trial (22 days).

The strength of this study was its ability to correlate PET findings in a homogenous group of patients to histopathologic findings after primary RPLND in a prospective fashion. Entry into the SEMS clinical trial requires that all patients have pure seminoma, retroperitoneal lymphadenopathy ≤ 3 cm on CT, were chemotherapy naïve, and underwent primary RPLND based on conventional imaging and expert surgical/multidisciplinary judgement. Importantly, PET scans were performed in parallel to conventional imaging, and treatment decisions were made based on conventional imaging and clinical expertise. Therefore, the risk of the PET findings resulting in selection or treatment bias was minimal.

Although adoption of PET imaging in primary seminoma is not recommended, this study had several notable findings. There was good correlation between the PET and intraoperative lymph node mapping in 84% of cases. This finding may eventually prove helpful in surgical planning as the optimal template in seminoma has yet to be defined and differences in nodal distribution have been described.¹³ Although RPLND in early metastatic seminoma is in its nascent stages, some have opted for a bilateral dissection in most cases. PET performed poorly in detecting the number of positive

lymph nodes with the number of PET-positive lymph nodes correlating with pathology in just half of cases. This was especially true in those with a second positive lymph node metastatic deposit ≤ 1 cm and argues for high-quality axial imaging to better determine the number of enlarged lymph nodes. Outside of the retroperitoneum and pelvis, PET findings in the chest, inguinal region, and tonsillar activity did not correlate with the presence of active cancer on follow-up. Suspicion for false-positive extraretroperitoneal lesions is needed in seminoma with a low volume metastatic burden.

The study, however, is not without limitations. The sample size ($n = 26$) is relatively small and not all patients on the SEMS trial underwent a PET scan. The time between RPLND and PET scan was variable and long in some patients. Finally, the determination of positive or negative imaging was based on local radiology. This methodology was chosen given the lack of consensus of what avidity defines a positive lymph node and a dearth of radiologists familiar with interpreting PET imaging in the primary setting. Central review could provide more uniform interpretation, although decrease the generalizability of the findings. Given the variations in PET utilization between academic and community centers, this emphasis on generalizability becomes accentuated.

The unmet need for a more accurate staging test in testicular seminoma is becoming more apparent. Recently, the Swedish Norwegian Testicular Cancer Study Group published favorable results of a prospective, large population-based study of RPLND as primary management of low volume clinical stage II seminoma.¹⁴ These findings add to 3 prospective clinical trials and signal a shift toward a surgical management of early metastatic seminoma.^{6,15,16} This change toward RPLND highlights both the understaging and overstaging of conventional imaging. The pN0 rates of in the prospective trials range from 3% to 16%, and subset of patients in these studies had more advanced disease than anticipated from clinical imaging. In SEMS, 44% had more advanced pathology than predicted and 5% were found to have pN3 disease.^{3,6} Not only does RPLND offer an alternative treatment with improved long-term morbidity compared with chemotherapy and radiotherapy, but histopathology serves as important feedback for clinical staging.

When discussing methods to improve diagnostic accuracy, it is important to consider new biology-based adjuncts to the novel biomarker miR371a-3p that is highly specific for GCTs and correlates with presence of active germ cell malignancy.¹⁷⁻¹⁹ SWE-NOTECA evaluated 24 patients with seminoma who underwent RPLND and found sensitivity of 74%, specificity of 100%, PPV of 100%, and NPV of 21%.²⁰ In the COTRIMS study, miR371a-3p predicted

active disease in 12/13 patients and benign disease in 3/3 cases.¹⁵ Other groups have reported on similar accuracy with miRNA in primary seminoma using RPLND histology.^{21,22} Large prospective investigations to define the biomarker's clinical utility are nearing completion. The miR371a-3p represents a possible noninvasive adjunct in predicting malignant retroperitoneal histology in germ cell tumors.

CONCLUSIONS

This study demonstrates favorable operational characteristics of 18F-FDG PET in detecting positive and negative retroperitoneal lymph nodes in patients with testicular retroperitoneal seminoma. The accuracy of PET seems to be similar to the predictive performance of conventional cross-sectional imaging and clinical expertise.

REFERENCES

- Stephenson A, Eggener SE, Bass EB, et al. Diagnosis and treatment of early stage testicular cancer: AUA guideline. *J Urol*. 2019;202(2):272-281. doi:10.1097/JU.0000000000000318
- Alsyouf M, Daneshmand S. Clinical stage II seminoma: management options. *World J Urol*. 2022;40(2):343-348. doi:10.1007/s00345-021-03854-8
- Farkouh A, Shete K, Cheng KW, Buell MI, Hu B. A systematic review of pN0 testicular seminoma: a new clinical entity and future directions. *Urol Oncol*. 2023;41(12):476-482. doi:10.1016/j.urolonc.2023.10.008
- Neuenschwander A, Lonati C, Antonelli L, et al. Treatment outcomes for men with clinical stage II nonseminomatous germ cell tumours treated with primary retroperitoneal lymph node dissection: a systematic review. *Eur Urol Focus*. 2023;9(3):541-546. doi:10.1016/j.euf.2022.11.003
- Alsyouf M, Nappi L, Nichols C, Daneshmand S. Plasma micro-RNA 371 expression in early-stage germ cell tumors: are we ready to move toward biology-based decision making?. *J Clin Oncol*. 2023;41(14):2478-2482. doi:10.1200/JCO.22.02002
- Daneshmand S, Cary C, Masterson T, et al. Surgery in early metastatic seminoma: a phase II trial of retroperitoneal lymph node dissection for testicular seminoma with limited retroperitoneal lymphadenopathy. *J Clin Oncol*. 2023;41(16):3009-3018. doi:10.1200/JCO.22.00624
- Pierorazio PM, Cheaib JG, Tema G, et al. Performance characteristics of clinical staging modalities for early stage testicular germ cell tumors: a systematic review. *J Urol*. 2020;203(5):894-901. doi:10.1097/JU.0000000000000594
- Cook GJ, Sohaib A, Huddart RA, Dearnaley DP, Horwich A, Chua S. The role of 18F-FDG PET/CT in the management of testicular cancers. *Nucl Med Commun*. 2015;36(7):702-708. doi:10.1097/MNM.0000000000000303
- Conduit C, Koh TT, Hofman MS, et al. Two decades of FDG-PET/CT in seminoma: exploring its role in diagnosis, surveillance and follow-up. *Cancer Imaging*. 2022;22(1):58. doi:10.1186/s40644-022-00496-w
- Albers P, Bender H, Yilmaz H, Schoeneich G, Biersack HJ, Mueller SC. Positron emission tomography in the clinical staging of patients with stage I and II testicular germ cell tumors. *Urology*. 1999;53(4):808-811. doi:10.1016/s0090-4295(98)00576-7
- Hain SF, O'Doherty MJ, Timothy AR, Leslie MD, Partridge SE, Huddart RA. Fluorodeoxyglucose PET in the initial staging of germ cell tumours. *Eur J Nucl Med*. 2000;27(5):590-594. doi:10.1007/s002590050547
- Wakileh GA, Ruf C, Heidenreich A, et al. Contemporary options and future perspectives: three examples highlighting the challenges in testicular cancer imaging. *World J Urol*. 2022;40(2):307-315. doi:10.1007/s00345-021-03856-6
- Zeng J, McFadden J, Thakker P, Tachibana I, Masterson TA, Cary C. Retroperitoneal nodal distribution for metastatic seminoma: is modified template appropriate? A retrospective study. *J Urol*. 2025;213(6):753-765. doi:10.1097/JU.0000000000004483
- Thor A, Negaard HFS, Grenabo Bergdahl A, et al. Primary retroperitoneal lymph node dissection as treatment for low-volume metastatic seminoma in a population-based cohort: the Swedish Norwegian Testicular Cancer Group experience. *Eur Urol Open Sci*. 2024;65:13-19. doi:10.1016/j.euro.2024.05.006
- Heidenreich A, Paffenholz P, Hartmann F, Seelemeyer F, Pfister D. Retroperitoneal lymph node dissection in clinical stage IIA/B metastatic seminoma: results of the Cologne Trial of Retroperitoneal Lymphadenectomy in Metastatic Seminoma (COTRIMS). *Eur Urol Oncol*. 2024;7(1):122-127. doi:10.1016/j.euo.2023.06.004
- Hiester A, Che Y, Lusch A, et al. Phase 2 single-arm trial of primary retroperitoneal lymph node dissection in patients with seminomatous testicular germ cell tumors with clinical stage IIA/B (PRIMETEST). *Eur Urol*. 2023;84(1):25-31. doi:10.1016/j.eururo.2022.10.021
- Gillis AJ, Rijlaarsdam MA, Eini R, et al. Targeted serum miRNA (TSmiR) test for diagnosis and follow-up of (testicular) germ cell cancer patients: a proof of principle. *Mol Oncol*. 2013;7(6):1083-1092. doi:10.1016/j.molonc.2013.08.002
- Dieckmann KP, Radtke A, Spiekermann M, et al. Serum levels of microRNA miR-371a-3p: a sensitive and specific new biomarker for germ cell tumours. *Eur Urol*. 2017;71(2):213-220. doi:10.1016/j.eururo.2016.07.029
- Nappi L, Thi M, Lum A, et al. Developing a highly specific biomarker for germ cell malignancies: plasma miR371 expression across the germ cell malignancy spectrum. *J Clin Oncol*. 2019;37(33):3090-3098. doi:10.1200/JCO.18.02057
- Thor A, Myklebust MP, Grenabo Bergdahl A, et al. miR-371a-3p predicting viable tumor in patients undergoing retroperitoneal lymph node dissection for metastatic testicular cancer: the SWENOTECA-MIR study. *J Urol*. 2024;212(5):720-730. doi:10.1097/JU.0000000000004164
- Heidenreich A, Thor A, Kjellmann A, et al. MP01-08 MicroRNA-371a-3p (miR371a) serum levels to predict the presence of metastatic lymph nodes in marker negative clinical stage IIA/B seminoma. *J Urol*. 2024;211(5S):e4-e5. doi:10.1097/01.Ju.0001008660.87408.90.08
- Seelemeyer F, Pfister D, Pappesch R, Merkelbach-Bruse S, Paffenholz P, Heidenreich A. Evaluation of a miRNA-371a-3p assay for predicting final histopathology in patients undergoing primary nerve-sparing retroperitoneal lymphadenectomy for stage IIA/B seminoma or nonseminoma. *Eur Urol Oncol*. 2024;7(3):319-322. doi:10.1016/j.euo.2023.10.021

EDITORIAL COMMENT

Guidelines support 18-fluorodeoxyglucose (FDG) positron emission tomography (PET) scans only for retroperitoneal masses > 3 cm after chemotherapy

for seminoma. However, in clinical practice, PET scans are occasionally used in the primary workup despite limited supporting data. Anecdotally, this

seems to be more frequent when the initial workup is driven by medical oncology.

The Surgery in Early Metastatic Seminoma trial was a landmark effort validating primary retroperitoneal lymph node dissection (RPLND) for well-selected, low-volume metastatic pure seminoma patients.¹ Trial design allowed pretreatment PET scans at the discretion of the treating institution, offering an opportunity to explore their utility. Although the numbers are small and these data probably change very little in clinical practice, prospective, chemo-naïve retroperitoneal surgical data in pure seminoma are uncommon and deserve attention.

Notably, missed metastatic lymph nodes ranged in pathological size from 0.7 cm to 1 cm. This illustrates a potential weakness associated with PET imaging. As commented on in prior research by Chang et al,² lesions smaller than 1 cm might not show high 18F-FDG uptake and could contribute to rates of false negatives because of partial volume effect. The authors conclude that

PET scans correlate reasonably well with pathological specimens; however, comparisons to standard contrasted CT scans are challenging because of the absence of primary RPLND seminoma surgical data. We look forward to better examining this question as primary RPLND for early-stage seminoma becomes more common.

Others have described the utility of PET staging. Cook et al³ found that in patients with equivocal staging CT, a negative 18F-FDG PET was helpful in management decisions. However, we agree that this does not represent an endorsement for the use PET imaging solely for primary staging. Similarly, the data presented by Hu et al⁴ suggest that PET imaging may be useful as adjunct information and warrants further investigation as we adopt primary RPLND for stage I to II seminoma.

John C. Norton¹ and Charles C. Peyton¹

¹Department of Urology, The University of Alabama at Birmingham
Birmingham, Alabama

REFERENCES

1. Daneshmand S, Cary C, Masterson T, et al. Surgery in early metastatic seminoma: a phase II trial of retroperitoneal lymph node dissection for testicular seminoma with limited retroperitoneal lymphadenopathy. *J Clin Oncol*. 2023;41(16):3009-3018. doi:10.1200/JCO.22.00624
2. Chang JM, Lee HJ, Goo JM, et al. False positive and false negative FDG-PET scans in various thoracic diseases. *Korean J Radiol*. 2006;7(1):57-69. doi:10.3348/kjr.2006.7.1.57
3. Cook GJ, Sohaib A, Huddart RA, Dearnaley DP, Horwich A, Chua S. The role of 18F-FDG PET/CT in the management of testicular cancers. *Nucl Med Commun*. 2015;36(7):702-708. doi:10.1097/MNM.0000000000000303
4. Hu B, Alsyouf M, Farkouh A, et al. Accuracy of 18F-fluorodeoxyglucose positron emission tomography in early metastatic testicular seminoma: analysis from the SEMS trial. *J Urol*. 2025;214(3):272-279. doi:10.1097/JU.0000000000004561

Utility of Routine Preoperative ¹⁸F-Fluorodeoxyglucose Positron Emission Tomography/Computerized Tomography in Identifying Pathological Lymph Node Metastases at Radical Cystectomy



Shawn Dason, Nathan C. Wong,* Timothy F. Donahue, Andreas Meier, Junting Zheng, Lorenzo Mannelli, Pier Luigi Di Paolo, Lucas W. Dean, Victor A. McPherson, Jonathan E. Rosenberg, Dean F. Bajorin, Marinella Capeanu, Guido Dalbagni, H. Alberto Vargas and Bernard H. Bochner

From the Department of Urology (SD), The Ohio State University, Columbus, Ohio, Urology Service (NCW, TFD, LWD, VAM, GD, BHB), Department of Surgery, Department of Radiology (AM, LM, PLDP, HAV), Department of Epidemiology and Biostatistics (JZ, MC), Genitourinary Oncology Service (JER, DFB), Department of Medicine, Memorial Sloan Kettering Cancer Center, New York, New York

Abbreviations and Acronyms

cNO = clinically node negative
cN+ = clinically node positive
CT = computerized tomography
FDG = fluorodeoxyglucose
MIBC = muscle invasive bladder cancer
PET = positron emission tomography
PLND = pelvic lymph node dissection
pN+ = pathologically node positive
RC = radical cystectomy
SUVmax = maximum standardized uptake value

Purpose: We determined the diagnostic performance of ¹⁸F-FDG (fluorodeoxyglucose) positron emission tomography/computerized tomography for detecting nodal metastases in patients with muscle invasive urothelial bladder cancer before radical cystectomy.

Materials and Methods: Preoperative ¹⁸F-FDG positron emission tomography/computerized tomography scans (208) were retrospectively reviewed. Scans were routinely performed in 185 patients with muscle invasive urothelial bladder cancer between August 2012 and February 2017, all of whom underwent radical cystectomy and pelvic lymph node dissection. Analyses were stratified by clinical node involvement and chemotherapy status. The diagnostic performance of ¹⁸F-FDG positron emission tomography/computerized tomography was assessed according to sensitivity, specificity, positive predictive value and negative predictive value.

Results: Lymph node metastases at time of pelvic lymph node dissection were present in 21.8% of those without suspicious nodes on computerized tomography (clinically node negative) and 52.6% of those with suspicious nodes on computerized tomography (clinically node positive). Median metastatic focus size was 5 mm. In clinically node negative cases ¹⁸F-FDG positron emission tomography/computerized tomography rarely detected nodal metastases (sensitivity 7% to 23%). In clinically node positive cases negative ¹⁸F-FDG positron emission tomography/computerized tomography was useful in ruling out lymph node metastases (sensitivity 92% to 100%). This study was limited by its mixed population and focus on pelvic nodal metastases only.

Conclusions: ¹⁸F-FDG positron emission tomography/computerized tomography appears to be most useful for better characterization of enlarged nodes identified by computerized tomography. Routine preoperative ¹⁸F-FDG positron emission tomography/computerized tomography has limited utility in clinically node negative cases.

Key Words: neoplasm staging, positron-emission tomography, cystectomy, lymph node excision, urinary bladder neoplasms

Accepted for publication February 27, 2020.
Supported by the Sidney Kimmel Center for Prostate and Urologic Cancers and funded in part through the NIH/NCI Cancer Center Support Grant P30 CA008748.

No direct or indirect commercial, personal, academic, political, religious or ethical incentive is associated with publishing this article.

* Correspondence: (e-mail: Nathan.wong@medportal.ca).

^{18}F -FDG PET/CT is being increasingly used before radical cystectomy for staging of high risk bladder cancer. From 2004 to 2011 the proportion of patients with stage II or III bladder cancer undergoing ^{18}F -FDG PET/CT increased from 1% to 15% in the SEER (Surveillance, Epidemiology, and End Results) registry.¹ This increasing use of ^{18}F -FDG PET/CT occurred without endorsement by the American Urological Association² or European Association of Urology guidelines.³

The utility of ^{18}F -FDG PET/CT rests in its ability to potentially identify lymph node metastases before radical cystectomy. In the advanced stage setting, a study from our center found ^{18}F -FDG PET/CT to have a sensitivity of 92% with a specificity of 81% for lymph node metastases.⁴ Nonetheless, diagnostic properties in the metastatic setting may not necessarily apply to the radical cystectomy population due to a lower inherent metastatic burden. Current studies of ^{18}F -FDG PET/CT before radical cystectomy are summarized in a recent meta-analysis of 13 studies, among which the average number of patients was 49 and the average proportion with pathology confirmed lymph node metastases was 30%.⁵ Sensitivity ranged from 33% to 100% (n-weighted mean 55%) and specificity from 58% to 100% (n-weighted mean 93%). The wide ranges of these values result from the heterogeneous nature of these studies, which generally pooled patients regardless of preoperative chemotherapy status, nodal size on CT or extent of PLND. Based on these data it remains unclear whether ^{18}F -FDG PET/CT is useful before radical cystectomy and, if so, under which clinical circumstances.

Uncertainty surrounding the value of ^{18}F -FDG PET/CT in the radical cystectomy candidate led us to perform this study. From 2012 to 2017 we began routinely offering ^{18}F -FDG PET/CT before radical cystectomy in patients with high risk invasive bladder cancer. We conducted a re-review of these data by a dedicated genitourinary radiologist to determine the diagnostic accuracy of ^{18}F -FDG PET/CT in several distinct populations of patients who undergo radical cystectomy. Our goal was to assess whether routine ^{18}F -FDG PET/CT use had value and to more precisely define the population that would benefit.

METHODS

Eligibility Criteria and Patient Characteristics

Patients were eligible for study inclusion if they had MIBC and underwent ^{18}F -FDG PET/CT before radical cystectomy, and underwent a templated RC-PLND as described between August 2012 and February 2017. Patients were excluded if they had primary urethral cancer, nonurothelial bladder cancer, concurrent active malignancy other than MIBC, did not receive a templated extended PLND or underwent ^{18}F -FDG PET/CT more than 60 days before RC-PLND or chemotherapy.

Planned stratifications for this study included clinical node status (cN0 or cN+) and timing of ^{18}F -FDG PET/CT relative to chemotherapy (pre-chemotherapy, post-chemotherapy and no chemotherapy). cN+ disease was defined as the presence of an enlarged pelvic lymph node with short-axis diameter of 10 mm or greater on a conventional CT with contrast performed before PET/CT. Conventional CT and ^{18}F -FDG PET/CT were interpreted by a genitourinary radiologist at our institution.

^{18}F -FDG Positron Emission Tomography/Computerized Tomography

^{18}F -FDG was administered intravenously approximately 60 minutes before imaging on dedicated PET/CT scanners (GE Medical Systems, Waukesha, Wisconsin) from the mid skull to the mid thigh. Images were obtained for 3 to 5 minutes per bed position depending on patient size. All ^{18}F -FDG PET/CT studies were reviewed and annotated in detail for the purpose of this study by an experienced genitourinary radiologist using picture-archiving workstations that display CT, PET and PET/CT fusion image sets in various orthogonal planes. SUVmax, normalized to patient lean body mass, were recorded using a 3-dimensional tool placed over sites of abnormal ^{18}F -FDG uptake. ^{18}F -FDG PET/CT findings were characterized as abnormal/suspicious for malignancy if uptake intensity was greater than that of adjacent blood pool or normal gluteal muscle activity (background) and not explained by physiological processes (eg urinary ^{18}F -FDG excretion in the ureters/bladder). The locations of all areas of suspicious radiotracer uptake were recorded and cataloged.

Pathological Assessment of Lymph Nodes

All patients underwent RC-PLND. The templated PLND involved bilateral removal of all nodal tissue with associated fibroadipose tissue and skeletonization of vessels from the genitofemoral nerve laterally, node of Cloquet caudally, pelvic floor inferiorly and cranially to include at least the aortic bifurcation. Additional lymph nodes in the presacral space and fossa of Marcellie were also removed. Lymph nodes were sorted by anatomical region (right common iliac, left common iliac, right pelvic, left pelvic, presacral and para-aortic nodes) and submitted for pathology separately to ensure detailed evaluation and accurate mapping.

Pathological specimens were processed and reviewed in the standard fashion by an experienced genitourinary pathologist. The number of positive lymph nodes in addition to the total number of lymph nodes was reported in each anatomical region. The diameter of the largest metastatic lesion in each region was also measured.

Statistical Analysis

The sensitivity, specificity, positive predictive value and negative predictive value were calculated for ^{18}F -FDG PET/CT detection of pathologically positive lymph nodes on a per patient (a positive PET in a patient with pN+) and per anatomical region (whether the site on PET positive finding was in the region of a pathologically positive node) basis among patients with clinically node negative disease, defined as lymph nodes less than 10 mm short axis on preoperative CT. The regional analysis was conducted to more accurately identify the diagnostic properties of PET/CT by reducing chance associations that might

relate to analysis on a patient level. Confidence intervals were estimated based on the Rao-Scott method to take into account multiple scans per patient.⁶ We did not re-review baseline CT of patients included in our previous report on the diagnostic properties of ¹⁸F-FDG PET/CT for patients with nodal metastatic disease,⁴ nor did we perform a per region analysis among patients with cN+ disease. All statistical analyses were performed in software packages SAS® 9.4 or R version 3.4 (The R Foundation for Statistical Computing).

RESULTS

Patient Characteristics

The study cohort comprised 185 patients, from whom 208 ¹⁸F-FDG PET/CT scans were collected and analyzed. Baseline characteristics are detailed in table 1. Most (170, 82%) scans were from patients classified as having cN0 disease based on CT and 38 (18%) were from those classified by CT as having cN+ disease.

Among patients with cN0 disease nodal metastases were pathologically confirmed (pN+) after surgery in 21.8%, compared with 52.6% of those with cN+ disease. In pN+ cases the median metastatic focus size was 5 mm and a median of 2 nodes were positive.

Diagnostic Characteristics of ¹⁸F-FDG PET/CT

Among patients with cN0 disease (170 scans) ¹⁸F-FDG PET/CT had very poor sensitivity for detecting nodal metastases, ranging from 7% in patients who had received chemotherapy before imaging to 23% in those who had not yet received

chemotherapy. However, its specificity was high, ranging from 89% to 99% (table 2). This finding was consistent across all subgroups of patients regardless of chemotherapy status or whether the analysis was conducted on a per patient or per region basis. Similarly, the positive predictive value was low (25% to 37%) and the negative predictive value was modest (7% to 83%) on a per patient level.

Our cohort included 38 patients with cN+ disease (table 1). Among the 13 patients who did not receive preoperative chemotherapy ¹⁸F-FDG PET/CT had a sensitivity of 100% (95% CI 47.8–100) and a specificity of 62.5% (95% CI 20.8–91) for detecting nodal metastases. We did not evaluate the diagnostic performance of pre-chemotherapy and post-chemotherapy scans due to the potential confounding effects of chemotherapy exposure on imaging findings and final pathology in the setting of a limited number of events (supplementary table 1, <https://www.jurology.com>).

Pre-Chemotherapy and Post-Chemotherapy PET/CT Analysis

To determine if either stability or a change in metabolic response could predict negative final pathology, we analyzed the ¹⁸F-FDG PET/CT scans of 23 patients who underwent imaging before and after preoperative chemotherapy (supplementary figure, <https://www.jurology.com>). We found no evidence that either metastatic lesion stability or change in metabolic response correlated with pN+ status. In this exploratory analysis the rate of

Table 1. Patient, disease and preoperative chemotherapy characteristics

	cN0		cN+	
	<i>Pt characteristics</i>			
Median age (IQR)	67	(59–74)	67	(59–74)
No. female (%)	32	(19)	8	(21)
	<i>Disease characteristics</i>			
No. pathological tumor stage at cystectomy (%):				
T0	28	(16)	3	(8)
Tis	18	(11)	3	(8)
Ta	2	(1)	1	(3)
T1	5	(3)	1	(3)
T2	37	(22)	6	(16)
T3	77	(45)	23	(61)
T4	3	(2)	1	(3)
Median lymph node count (IQR)	28	(20–37)	36	(23–49)
No. pN+ disease (%)	37	(22)	20	(53)
Median pos node count (IQR)	2	(1–6)	2	(2–5)
Median cm largest metastatic focus in pN+ cases (IQR)	0.5	(0.2–0.9)	0.6	(0.3–0.8)
	<i>Preop chemotherapy characteristics</i>			
No. preop chemotherapy received (%)	114	(67)	25	(66)
No. chemotherapy regimen (%):				
Gemcitabine + cisplatin	97	(85)	18	(72)
Other	17	(15)	7	(28)
No. scan timing relative to chemotherapy (%):				
No chemotherapy	56	(33)	13	(34)
PET/CT before chemotherapy	60	(35)	18	(47)
PET/CT after chemotherapy	54	(32)	7	(18)
Median days PET/CT to first chemotherapy dose (IQR)	13	(7–21)	15	(10–22)
Median days from last chemotherapy dose to PET/CT (IQR)	28	(14–42)	32	(24–51)

Table 2. Diagnostic properties of ^{18}F -FDG PET/CT for detecting nodal metastases in patients without abnormal nodes on CT

	Sensitivity (%)	95% CI	Specificity (%)	95% CI	Pos Predictive Value (%)	95% CI	Neg Predictive Value (%)	95% CI
Per pt:								
No chemotherapy	10.0	0.8–58.0	93.5	80.9–98.0	25.0	0.4–96.0	82.7	69.4–91.0
Post-chemotherapy	7.1	0.7–44.0	95.0	81.1–99.0	33.3	0.0–100.0	74.5	60.4–85.0
Pre-chemotherapy	23.0	6.3–57.0	89.4	76.2–96.0	37.5	8.6–79.0	80.8	67.3–90.0
Per region:								
No chemotherapy	9.0	0.8–53.0	98.7	96.6–100.0	33.3	2.0–92.0	93.9	87.8–96.0
Post-chemotherapy	Not applicable	Not applicable	99.0	96.9–100.0	Not applicable	Not applicable	91.3	85.2–95.0
Pre-chemotherapy	10.0	0.9–55.0	98.5	96.0–99.0	20.0	0.7–89.0	96.6	93.3–98.0

discrepant findings ranged from 33% (pathologically confirmed metastases following stable negative PET/CT) to 100% (no metastatic lymph nodes after conversion from negative to positive PET/CT).

Incidental Findings

To better understand the implications of routinely performing ^{18}F -FDG PET/CT before RC-PLND we assessed the incidental findings identified in patients not receiving chemotherapy (69). We excluded patients receiving chemotherapy because they received multiple imaging tests and we could not ascribe the origin of the incidental findings. Numerous investigations and procedures were prompted by ^{18}F -FDG PET/CT detected lesions (supplementary table 2, <https://www.jurology.com>). Two unrelated malignancies were diagnosed and it is uncertain if these would have been detected by conventional modalities.

DISCUSSION

Routine ^{18}F -FDG PET/CT was not useful in identifying lymph node metastases in patients with cN0 disease on CT. This finding arises from the observed low sensitivity (7% to 23%) in this group. The low sensitivity is likely a result of the low burden of disease in these patients, where the median metastatic focus size within the involved lymph node was only 5 mm.

The main use of ^{18}F -FDG PET/CT is likely in better evaluating clinically suspicious lymph nodes identified by conventional CT. We found that a negative ^{18}F -FDG PET/CT in this group ruled out lymph node metastases due to the high sensitivity of ^{18}F -FDG PET/CT in this group. Our findings corroborate those of an earlier study from our center supporting the high sensitivity of ^{18}F -FDG PET/CT in patients with lymph node metastases.⁴ Among 51 suspicious lymph nodes on ^{18}F -FDG PET/CT, sensitivity was 92% (95% CI 74–99) and specificity was 81% (95% CI 61–93). Together these results indicate that a suspicious lymph node identified on CT that is not PET-avid can be presumed to be pathologically negative. Management of a PET-avid suspicious node is less clear. Other risk factors along with the degree of certainty required for clinical decision making will influence whether this is presumed to be truly positive or a percutaneous

biopsy is performed. Alternatively, those with a PET-avid node could receive a preoperative chemotherapy regimen that does not differ based on suspicion of metastatic disease, such as 6 cycles of dose-dense gemcitabine and cisplatin.⁷

We did not find any suggestion that ^{18}F -FDG PET/CT had clinical utility in any other scenarios that we studied. Post-chemotherapy scans have exceedingly low sensitivity and positive predictive value, preventing their use in informing decisions on whether to perform consolidative RC-PLND. Additionally, we saw no evidence that either stable ^{18}F -FDG PET/CT findings before and after chemotherapy or conversion from positive to negative predicted pN+ status. These findings all reaffirm extended PLND as the only accurate lymph node staging method presently available for patients with MIBC.

Data prior to our study were presented in a recent meta-analysis of 13 studies, demonstrating a wide range of sensitivities from 33% to 100% and specificities from 58% to 100%.⁵ We hypothesize that these heterogeneous findings are likely attributable to differences in study design. By separately analyzing data from cN0 and cN+ cases, we identified major differences in sensitivity, allowing clear conclusions regarding clinical utility in these distinct settings. This is a practical stratification because clinical nodal status is generally known before ^{18}F -FDG PET/CT. Other strengths of our investigation included the lack of selection bias resulting from routine use of ^{18}F -FDG PET/CT during this period and consistent re-review of all scans by a dedicated genitourinary radiologist.

This study was limited by the mixed population with respect to chemotherapy exposure and the timing of ^{18}F -FDG PET/CT relative to chemotherapy. Chemotherapy could impact our findings if lymph nodes completely responded, leading to pathologically node negative status despite positive ^{18}F -FDG PET/CT findings. Nonetheless, we do not believe this limitation impacts our overall conclusions. We were also limited in our ability to assess the utility of ^{18}F -FDG PET/CT in detecting distant metastases before RC-PLND. This limitation arises from the fact that these patients would ultimately not undergo radical cystectomy and, thus, not be included in our study cohort. Finally, we were limited in our ability

to assess the value of SUVmax in distinguishing positive from negative lymph nodes because of study size. As a higher SUVmax PET lesion is more likely to be pathologically positive,⁸ a higher cutoff could improve specificity. The ideal SUVmax cutoff should be defined in future research.

One of the broader implications of this study is that routine ¹⁸F-FDG PET/CT in the radical cystectomy candidate, particularly with clinically negative lymph nodes, is unnecessary. Most patients with MIBC will have already undergone conventional CT, which is more widely available, less expensive, involves lower radiation exposure and has a shorter acquisition time compared with ¹⁸F-FDG PET/CT. Additionally,

¹⁸F-FDG PET/CT leads to a higher rate of incidental findings, prompting more invasive investigations, anxiety and costs. Thus, ¹⁸F-FDG PET/CT use should be limited to patients in whom it has clinical utility, namely those with abnormal nodes on CT.

CONCLUSIONS

¹⁸F-FDG PET/CT should not be used as a routine test before radical cystectomy. Its main utility is in evaluating equivocal lymph nodes seen on conventional CT. Further research is required to clarify the role of ¹⁸F-FDG PET/CT in assessing chemotherapy response.

REFERENCES

- Huo J, Chu Y, Chamie K et al: Increased utilization of positron emission tomography/computed tomography (PET/CT) imaging and its economic impact for patients diagnosed with bladder cancer. *Clin Genitourinary Cancer* 2018; **16**: e99.
- Chang SS, Bochner BH, Chou R et al: Treatment of non-metastatic muscle-invasive bladder cancer: AUA/ASCO/ASTRO/SUO guideline. *J Urol* 2017; **198**: 552.
- Witjes JA, Bruins M, Comp erat E et al: EAU guidelines on muscle-invasive and metastatic bladder cancer. Arnhem, The Netherlands: EAU Guidelines Office 2018.
- Apolo AB, Riches J, Sch oder H et al: Clinical value of fluorine-18 2-fluoro-2-deoxy-D-glucose positron emission tomography/computed tomography in bladder cancer. *J Clin Oncol* 2010; **28**: 3973.
- Crozier J, Papa N, Perera M et al: Comparative sensitivity and specificity of imaging modalities in staging bladder cancer prior to radical cystectomy: a systematic review and meta-analysis. *World J Urol* 2018; **37**: 1.
- Rao JN and Scott AJ: On chi-squared tests for multiway contingency tables with cell proportions estimated from survey data. *Ann Stat* 1984; **12**: 46.
- Iyer G, Balar AV, Milowsky MI et al: Multicenter prospective phase II trial of neoadjuvant dose-dense gemcitabine plus cisplatin in patients with muscle-invasive bladder cancer. *J Clin Oncol* 2018; **36**: 1949.
- Vind-Kezunovic S, Bouchelouche K, Ipsen P et al: Detection of lymph node metastasis in patients with bladder cancer using maximum standardised uptake value and 18F-fluorodeoxyglucose positron emission tomography/computed tomography: results from a high-volume centre including long-term follow-up. *Eur Urol Focus* 2019; **5**: 90.

EDITORIAL COMMENT

For many solid organ tumors ¹⁸F-FDG PET/CT (PET/CT) sensitivity is superior to conventional CT, making it part of the routine staging assessment.¹ Perhaps by extrapolation PET/CT for bladder cancer is on the rise despite absence of supporting data. In fact, PET/CT has become so universally ensconced in clinical practice that patients question the thoroughness of their evaluation if they have not had one. Dason et al retrospectively examined 208 patients with muscle invasive urothelial cancer who underwent PET/CT prior to radical cystectomy with extended pelvic lymph node dissection between 2012 and 2017. Two-thirds of the cohort received neoadjuvant chemotherapy.

Overall 82% had clinically negative nodes on conventional CT imaging. Of these, 22% were found to have occult pathological nodal disease at time of surgery. The sensitivity of PET/CT for detecting occult disease ranged from a dismal 7% after chemotherapy

to only 23% for those without prior chemotherapy. The authors conclude that, unlike with other solid organ tumors, PET is not indicated in the setting of a normal conventional CT. This finding should inform more efficient and responsible use of health care dollars.

In contrast, of 13 patients who had suspicious nodes on conventional CT without prior chemotherapy, only 52% were positive at surgery. PET/CT predicted positive nodes with 100% sensitivity and 62.5% specificity, suggesting that there may be a role for this minority to help identify patients unlikely to benefit from surgery. There remains an unmet need for accurate preoperative staging of bladder cancer and novel radiotracers represent a promising avenue of research toward this objective.



Jodi K. Maranchie
University of Pittsburgh
Pittsburgh, Pennsylvania

REFERENCE

- Gallamini A, Zwarthoed C and Borra A: Positron emission tomography (PET) in oncology. *Cancers (Basel)* 2014; **6**: 1821.

REPLY BY AUTHORS



Bladder cancer is one of the costliest cancers and understanding the nuances of appropriate imaging is necessary in our stewardship of limited health care resources. Our study demonstrates that the routine patient undergoing radical cystectomy is unlikely to benefit from ^{18}F -FDG PET/CT (PET/CT) for lymph node staging over conventional imaging. The best data for PET/CT are in the setting of suspected metastatic disease where the PET avidity of a CT visible lesion can provide clarity as to the nature of this lesion. A prior study from Memorial Sloan Kettering Cancer Center supported the utility of PET/CT in the metastatic setting due to its excellent diagnostic properties and clinical utility in guiding further therapy (reference 4 in article). Corroborating this, surveys showed that clinicians changed their planned management in 68% of cases based on the PET/CT findings.

Our study emphasizes that advances in muscle invasive bladder cancer imaging need to focus on

improving sensitivity for small lymph node metastases. This will be accomplished by either improving the scanner or the imaging agent. Digital PET/CT has shown some promise in improving PET/CT resolution.¹ Additionally, advances in urothelial carcinoma therapeutics targeting specific molecular alterations like FGFR-3 and Nectin-4 support the possibility of targeted urothelial carcinoma molecular imaging,^{2,3} a concept which has become standard in prostate cancer treatment. Shifting away from the nuclear medicine approach, other imaging modalities such as ultrasmall paramagnetic iron oxide particles and magnetic resonance imaging have been previously shown to improve detection of metastasis and may also leverage magnetic resonance imaging for local tumor staging.⁴ Our study reminds us that it will be essential that novel imaging modalities demonstrate a clear improvement over our current standard before they are widely adopted.

REFERENCES

1. Koopman D, van Dalen JA, Stevens H et al: Performance of digital PET compared to high-resolution conventional PET in patients with cancer. *J Nucl Med* 2020; doi:10.2967/jnumed.119.238105.
2. Loriot Y, Necchi A, Park SH et al: Erdafitinib in locally advanced or metastatic urothelial carcinoma. *N Engl J Med* 2019; **381**: 338.
3. Rosenberg JE, O'Donnell PH, Balar AV et al: Pivotal trial of enfortumab vedotin in urothelial carcinoma after platinum and anti-programmed death 1/programmed death ligand 1 therapy. *J Clin Oncol* 2019; **37**: 2592.
4. Birkhäuser FD, Studer UE, Froehlich JM et al: Combined ultrasmall superparamagnetic particles of iron oxide-enhanced and diffusion-weighted magnetic resonance imaging facilitates detection of metastases in normal-sized pelvic lymph nodes of patients with bladder and prostate cancer. *Eur Urol* 2013; **64**: 953.